OCT 21 1948

WIRELESS ENGINEER

THE JOURNAL OF RADIO RESEARCH & PROGRESS

OCTOBER 1948

VOL. XXV. TWO SHILLINGS AND SIXPENCE - - No. 301

'VISCONOL'

CATHODRAY CONDENSERS *for*

TELEVISION & OTHER HIGH VOLTAGE APPLICATIONS

This well-known range of high voltage condensers is now processed with a new impregnant—"Visconol," a highly viscous mineral oil, the development of which has been dictated by the increasingly stringent operational conditions to which modern equipment is subjected. Among the advantages provided by this new process are:—adequate voltage rating, low power factor, stability of dielectric, and power to withstand sharp-front short-time fleeting surges. The mechanical construction and unique sealing technique renders them normally impervious to breakdown or flashover. T.C.C. "VISCONOL" Cathodray Condensers should be first choice where exacting conditions are likely. List No. 132, showing a full and comprehensive range will be sent on receipt of 2½d. stamp.

CAPACITIES FROM 0.0005 - 1 MFD.
VOLTAGE RATINGS FROM 750-25,000 D.C.

TCC CONDENSERS—*A PRE-REQUISITE TO "BETTER LISTENING"*

THE TELEGRAPH CONDENSER CO. LTD.

RADIO DIVISION

NORTH ACTON · LONDON · W·3 Telephone. ACORN 0061

WIRELESS ENGINEER

Vol. XXV OCTOBER 1948 No. 301

Ionospheric Complexities

RECENT research indicates that the structure and action of the ionosphere is much more complicated than was previously supposed. It is seventeen years since the single Heaviside layer was replaced by two or three ionized layers. Our Editorial of September 1931 was entitled 'How many ionized layers?' Experiments in Bavaria had shown that all the observations could be explained by multiple reflection from a single layer at a height of about 100 km, but these tests were all made at a wavelength of 532.9 metres and we said that 'great caution should be exercised in comparing the results with those obtained at other wavelengths.' Professor Appleton, as he then was, had come to the conclusion that other ionized layers must exist at heights of two or three hundred kilometres, and subsequent experiments fully confirmed the existence of these layers.

In *Nature* of 3 July there is an article by J. A. Ratcliffe of the Cavendish Laboratory, Cambridge, entitled 'Diffraction from the Ionosphere and the Fading of Radio Waves.' Fading is usually due to interference between waves which have travelled from the transmitter to the receiver by different routes; if they arrive in phase the signal is strengthened, whereas, if they arrive 180 degrees out of phase the signal may practically vanish. It has been found, however, that when, by using a short pulse and a special type of receiving aerial, the ground wave is suppressed, and a single downcoming wave is received, fading still occcurs. The speed of fading is found to be roughly proportional to the frequency of the wave. It is also found that for vertical incidence the fading differs at two points about a wavelength apart.

Ratcliffe gives a very interesting analogy in the appearance of a street lamp on a bridge reflected from an irregularly-rippled stream to an observer standing nearby. The radio receiver is similarly acted on by a cone of rays from a diffuse scattering region in the ionosphere, but the theory advanced to account for the fading has little in common with the rippling stream. Ratcliffe assumes that the surface of the ionosphere is rough and may be regarded as made up of a number of scattering 'centres.' On the analogy of the rippling stream one might assume that these different 'centres' reflected the incident beams in different directions, but the explanation is much more ingenious.

The different parts of the ionospheric surface

1923—1948

With this issue *Wireless Engineer* celebrates its twenty-fifth anniversary. The first number appeared in October 1923, under the title *Experimental Wireless* which was later changed to *Experimental Wireless & Wireless Engineer*, and eventually became the present *Wireless Engineer* in September 1931.

These changes of title portray the gradually changing contents of the journal from the original experimental outlook to the present engineering standard. Accompanying this change the Abstracts & References section has grown in importance from its original 1½ pages to its present average of 21 pages a month. Originally compiled by the Editorial staff, Abstracts & References have been since June 1926, compiled by the Radio Research Board and reproduced by arrangement with the Department of Scientific & Industrial Research.

are assumed to be in continual random motion, so that while one part of the incident wave may be reflected from a surface at rest, neighbouring parts may be reflected from patches that are moving away from or towards the transmitter. It is assumed that the velocities v in the line of sight of the ionospheric patches or centres are distributed according to a Gaussian law with a root-mean-square velocity v_0. When a wave is reflected from a surface which is moving in the line of sight, there is a Doppler shift of frequency, an increase if the motion is towards the transmitter and a decrease if the motion is away from the transmitter, as given by the formula $f = f_0 (1 + 2v/c)$.

If there were only two patches, one at rest and the other moving in the line of sight with a velocity v, the received wave would be made up of two of slightly different frequencies f and f_0, and fading would occur due to the beating between the two waves at a frequency of $2v/\lambda$. The phenomenon is of course, much more complicated when there are a great number of reflected waves with every possible frequency in a band about the transmitted frequency, but by applying the Gaussian distribution law it is shown that fading will still occur. A number of experiments have been made on pulses reflected from the F region, the fading curves being recorded and analysed. At a frequency of 4 Mc/s the results indicated a r.m.s. velocity v_0 of 5 metres per second. Tests made on other occasions at 2 Mc/s and 100 kc/s indicated r.m.s. velocities of 0.5 and 1.0 m/s respectively. Calculation also shows that the rate at which the fading curve changes, expressed in terms of the mean amplitude, will be equal to $4v_0/\lambda$. Experiment confirms that the rate of fading is inversely proportional to λ; i.e., proportional to the frequency employed in the tests. Most of the experiments were made at vertical incidence, but tests at oblique incidence give results that can be explained in the same way. As Ratcliffe points out, when the waves are reflected at an upper layer the results are complicated by their passage through the lower layer, and the results of any calculation will depend very much on the assumptions made.

The theory outlined is only meant to be a first approximation to the truth, but it raises many questions as to the nature of the ionosphere, the cause, nature and distribution of its turbulence, and its variation from time to time. G. W. O. H.

RING-AERIAL SYSTEMS

Minimum Number of Radiators Required

By H. Page, M.Sc., A.M.I.E.E.

(Research Dept., Engineering Division, British Broadcasting Corporation.)

SUMMARY.—The properties of ring-aerial systems, especially types designed to have antifading properties, have been recently described. In the analysis it was assumed that an idealized ring, containing an infinitely large number of aerials, was used.

The minimum number of aerials required to simulate the idealized ring reasonably closely is now investigated theoretically, and the results of measurements in one practical case are described.

1. Introduction

In a previous article[1] the properties of ring-aerial systems were discussed. These consist of a number of aerials, arranged in the form of a ring, the radius of which is comparable with the wavelength, λ.

In one arrangement, which will be referred to as the phased ring-aerial system, the amplitudes of the currents in all the aerials forming the ring are the same, but the phase changes progressively round the ring, the total phase change being an integral multiple of 2π radians, say $2\pi n$ radians where n is integral.

It was shown that the vertical polar diagram of the phased-ring system, assuming the individual aerials are short compared with λ, is given by:

$$E_\theta = \frac{J_n (q \sin \theta) \,.\, \sin \theta}{J_n(q)} \qquad \ldots \quad \ldots \quad (1)$$

where E_θ is the relative field strength at an angle θ to the vertical, and is made unity at $\theta = 90°$ for comparison purposes. $J_n(z)$ is the Bessel function of the first kind and order n, while $q = 2\pi r/\lambda$, r being the ring radius.

Typical vertical radiation diagrams are shown in Fig. 1, for a ring radius of 0.25λ and various values of n. For comparison purposes, in the same figure the dotted curve shows the vertical diagram of a single aerial. It is seen that,

MS accepted by the Editor, July 1947

compared with a single aerial, the arrangement in the form of a ring considerably decreases radiation at small values of θ, thus giving anti-fading properties. The vertical radiation diagram improves progressively as n increases.

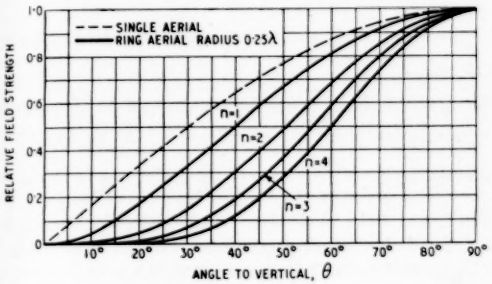

Fig. 1. *Vertical radiation diagram of phased ring-aerial system; total phase change round ring = $2\pi n$ radians.*

In a second type of ring-aerial system the ring currents are in phase, and a single aerial is added at the centre of the ring, carrying a current in phase with, or in phase opposition to, that of the ring aerials, depending on the ring radius; this type will be referred as the concentric ring-aerial system.

The expression for the vertical polar diagram, for aerials short compared with λ, has been shown to be[1]

$$E_\theta = \frac{\{k + J_0(q \sin \theta)\} \sin \theta}{\{k + J_0(q)\}} \quad \ldots \quad \ldots \quad (2)$$

where k is the ratio of the central aerial current to the total ring-aerial current.

Typical vertical-radiation diagrams are shown in Fig. 2, for a ring radius of 0.25λ and three typical values of k. These diagrams are similar to those for aerials between 0.5λ and 0.6λ high, such as are normally used for medium-wave broadcasting on account of their antifading properties.

In the analysis on which the previous results are based it is assumed that there is an infinitely large number of aerials in the ring. In this case the horizontal polar diagram is circular, and the vertical polar diagrams for the two arrangements are given by expressions (1) and (2) respectively.

It is, of course, not practicable to use an infinitely large number of aerials in the ring, and it becomes necessary to know the minimum number which can be used, while simulating the idealized ring reasonably closely. The effect of the finite number of aerials will be considered from two points of view. First, there will be a cyclical deviation of field strength in different directions along the ground, the horizontal polar diagram being serrated instead of circular. Secondly, there will be some distortion of the vertical polar diagram, which will vary in different directions from the aerial. Both these effects must be reduced to a negligible amount, and we will proceed to calculate the minimum number of aerials required to achieve this object.

In a practical case one other consideration may affect the choice of the number of aerials—the necessity of obtaining a relatively high radiation resistance for individual aerials. This may require an increase in the number of aerials above that required from the point of view of the preservation of the polar diagram shape; reference will be made to this point later.

2. Minimum Number of Ring Aerials

2.1 *Phased-Ring Aerial*

The minimum number of aerials required in the phased ring has been stated by Chireix,[2] but no proof was given. We will, therefore, prove this result first, in order to apply it later to the concentric ring-aerial system, for which the conclusions are somewhat different.

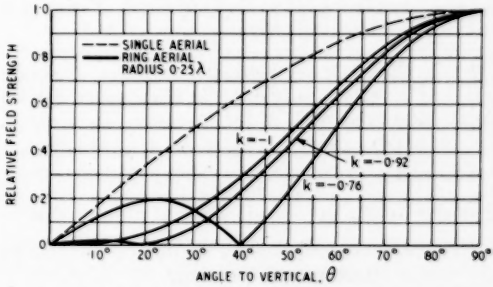

Fig. 2. *Vertical radiation diagram of concentric ring-aerial system.*

Fig. 3 shows s vertical aerials, A_1, A_2, . . . A_x, . . . A_s, equally spaced round the circumference of the ring, centre O and radius r. The aerial currents are equal and the phase angle lags progressively round the ring in a clockwise direction; the total phase change is $2\pi n$ radians.

We shall calculate the field strength at a point P, the distance OP, d being so large that $r/d \ll 1$. OC is perpendicular to the projection of OP in the horizontal plane. Calling α the angle between OA_s and OC, the angle between OA_x and OC is $\left(\frac{2\pi x}{s} - \alpha\right) = \beta$, say.

Let $E_\theta \sin(\omega t + \phi)$ be the field strength at P due to a vertical aerial, A_0, placed at O; here ω is the angular frequency and ϕ is an arbitrary

phase angle. A_0 is assumed to be of the same height as each of the aerials in the ring (and so to have the same vertical polar diagram) and to carry s times the current of each ring aerial.

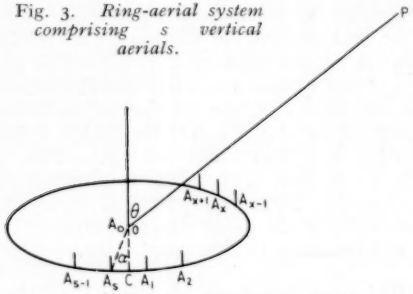

Fig. 3. *Ring-aerial system comprising s vertical aerials.*

Further, the phase of the current in A_0 is assumed the same as that in the aerial which would be at C in the idealized ring, containing an infinite number of aerials.

$$= \frac{E_\theta}{s} \sin(\omega t + \phi) \left\{ \sum_{u=0}^{\infty} J_u(q \sin\theta) \sum_{x=1}^{s} \cos(n-u)\beta + \sum_{u=1}^{\infty} (-1)^u J_u(q \sin\theta) \sum_{x=1}^{s} \cos(n+u)\beta \right\}$$

$$- \frac{E_\theta}{s} \cos(\omega t + \phi) \left\{ \sum_{u=1}^{\infty} J_u(q \sin\theta) \sum_{x=1}^{s} \sin(n-u)\beta + \sum_{u=1}^{\infty} (-1)^u J_u(q \sin\theta) \sum_{x=1}^{s} \sin(n+u)\beta \right\}$$

E_θ is the relative field strength for a single aerial at a vertical angle θ; in the case of aerials short compared with λ, for instance, $E_\theta = \sin\theta$.

Now $PO - PA_x \approx r \sin\theta \sin\beta$, as $r/d \ll 1$.

The phase of the field due to A_x therefore leads that due to A_0 by $\frac{2\pi r}{\lambda} \sin\theta \sin\beta$ radians due to path difference, and lags by $n\beta$ due to the change of current phase round the ring.

The field strength at P due to A_x therefore becomes :

$$\frac{E_\theta}{s} \sin\left\{\omega t + \phi + q \sin\theta \sin\beta - n\beta\right\}$$

where $q = \frac{2\pi r}{\lambda}$

$$= \frac{E_\theta}{s} \sin(\omega t + \phi) \cos(q \sin\theta \sin\beta - n\beta) + \frac{E_\theta}{s} \cos(\omega t + \phi) \sin(q \sin\theta \sin\beta - n\beta) \quad .. \quad .. \quad .. \quad (3)$$

We next make use of the following relationships due to Anger* :

$$\cos(z \sin\beta) = J_0(z) + 2 \sum_{u=1}^{\infty} J_{2u}(z) \cos 2u\beta \quad .. \quad .. \quad .. \quad (4)$$

and $$\sin(z \sin\beta) = 2 \sum_{u=1}^{\infty} J_{2u-1}(z) \sin(2u-1)\beta \quad .. \quad .. \quad .. \quad .. \quad (5)$$

to obtain

$$\cos(q \sin\theta \sin\beta - n\beta) = \cos(q \sin\theta \sin\beta) \cos n\beta + \sin(q \sin\theta \sin\beta) \sin n\beta = \sum_{u=0}^{\infty} J_u(q \sin\theta) \cos(n-u)\beta + \sum_{u=1}^{\infty} (-1)^u J_u(q \sin\theta) \cos(n+u)\beta.$$

Similarly,

$$\sin(q \sin\theta \sin\beta - n\beta) = \sin(q \sin\theta \sin\beta) \cos n\beta - \cos(q \sin\theta \sin\beta) \sin n\beta = -\sum_{u=0}^{\infty} J_u(q \sin\theta) \sin(n-u)\beta - \sum_{u=0}^{\infty} (-1)^u J_u(q \sin\theta) \sin(n+u)\beta.$$

The total field at P due to all the ring aerials is obtained by summing these contributions, for values of x from 1 to s. This gives :

$$\frac{E_\theta}{s} \sin(\omega t + \phi) \sum_{x=1}^{s} \cos(q \sin\theta \sin\beta - n\beta) + \frac{E_\theta}{s} \cos(\omega t + \phi) \sum_{x=1}^{s} \sin(q \sin\theta \sin\beta - n\beta)$$

Now when $\beta = \left(\frac{2\pi x}{s} - \alpha\right)$,

$\sum_{x=1}^{s} \cos(n \pm u)\beta = s \cos(ps\alpha)$ when $\left(\frac{n \pm u}{s}\right)$ is equal to an integer p, positive, negative or zero, and o for all other values of $\left(\frac{n \pm u}{s}\right)$.

Also $\sum_{x=1}^{s} \sin(n \pm u)\beta = -s \sin(ps\alpha)$ when $\left(\frac{n \pm u}{s}\right)$ is equal to an integer p, positive, negative or zero, and o for all other values of $\left(\frac{n \pm u}{s}\right)$.

Inserting these results in the expression for the total field at P, and arranging the terms in increasing order of the Bessel coefficients, it follows that in order to simulate the ideal ring and make $J_n(q \sin\theta)$ the first term with a non-zero coefficient, s must be greater than $2n$.

The next most important term occurs when $u = (s - n)$, and is equal to :

$$(-1)^{s-n} E_\theta J_{(s-n)}(q \sin\theta) \{\sin(\omega t + \phi) \cos s\alpha + \cos(\omega t + \phi) \sin s\alpha\} = (-1)^{s-n} E_\theta \sin(\omega t + \phi + s\alpha) J_{s-n}(q \sin\theta).$$

The terms involving higher order Bessel coefficients are negligible in comparison with this, which may be considered the dominant deviation

* G. N. Watson, Theory of Bessel Functions, (Cambridge, 1922), Section. 2.22.

term due to the use of a finite number of aerials in the ring.

The maximum value of this term occurs when $s\alpha = 0$ and π and is then equal to :

$$\pm E_\theta \sin(\omega t + \phi) J_{(s-n)}(q \sin\theta),$$

having one complete cycle between adjacent aerials. The horizontal polar diagram, instead of being circular as it is for the idealized ring, is therefore serrated, there being one complete cycle of deviation between adjacent aerials. If s exceeds n by an even number, there will be polar-diagram maxima in the direction of individual aerials ; if s exceeds n by an odd number there will be polar-diagram minima in the direction of individual aerials.

The maximum deviation from the mean expressed as a ratio is

$$\frac{\pm J_{(s-n)}(q \sin\theta)}{J_n(q \sin\theta)} \quad .. \quad .. \quad .. \quad (6)$$

Along the ground, when θ is 90°, this reduces to

$$\frac{\pm J_{(s-n)}(q)}{J_n(q)} \quad .. \quad .. \quad .. \quad (7)$$

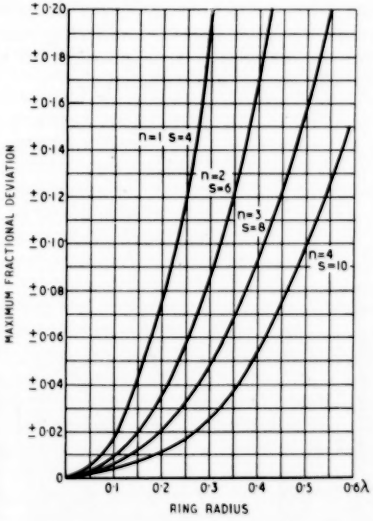

Fig. 4. *Maximum deviation of field strength along ground of phased ring-aerial system. Total phase change round ring = $2\pi n$ radians ; number of aerials in ring = s.*

Fig. 4 shows the value of the deviation term for different values of n and s, s being chosen to make the deviation reasonably small over the range of ring radii considered. At first sight it may appear that for the larger values of n in Fig. 4 a smaller value of s might be used. However, reduction of the total number of aerials by only one makes the fractional deviation prohibitively great. For instance, when the ring radius is 0.35λ and n is 2 the deviation is $\pm$ 0.12 for $s = 6$ but $\pm$ 0.41 for $s = 5$. A further point to be borne in mind is that for the higher values of n it is necessary to use larger ring radii in order to obtain a reasonable value of radiation resistance[1].

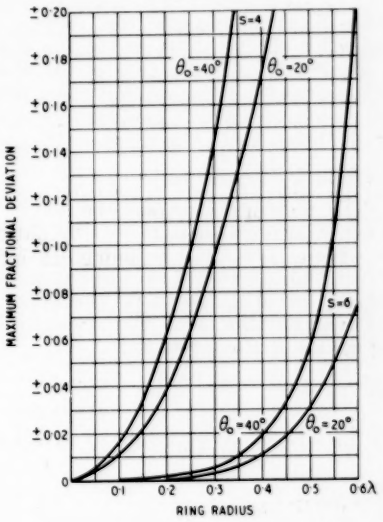

Fig. 5. *Maximum deviation of field strength along ground (s even) for concentric ring-aerial system ; number of aerials in ring = s.*

A complete consideration of the best compromise to be adopted is outside the scope of this paper. For a typical case, however, it turns out that four ring aerials would be satisfactory when $n = 1$, and lead to a reasonable value for the radiation resistance for individual ring aerials, and a fractional deviation of field strength along the ground of $\pm$ 0.1, or $\pm$ 10%. When $n = 2$, six aerials are satisfactory, but for higher values of n, values of s greater than 8 and 10 respectively would be required. Whether such a complicated system is worth while for the improvement in vertical-radiation diagram shown in Fig. 1 is too involved a question to be considered here.

The maximum fractional deviation decreases continuously as s increases, so the greater the number of aerials the more closely is a circular horizontal polar diagram approached. This is not the case for the concentric ring-aerial system, as we shall see later.

A further point to be noted is that, for the range of ring radii in which we are interested,

when q is less than the first positive value of z for which $J_n(z)$ is maximum,

$$\frac{J_{(s-n)}(q \sin \theta)}{J_n(q \sin \theta)} < \frac{J_{(s-n)}(q)}{J_n(q)}$$

At all values of θ, therefore, we have fluctuations of field strength from the mean, the percentage fluctuation increasing progressively with θ, being greater along the ground than at small values of θ. This means that in the direction of the polar-diagram maxima the vertical polar diagram will be better than, and in the direction of the minima worse than, that of the idealized ring. The change in the vertical polar diagram in different directions will, however, be small, if that of the horizontal polar diagram is small.

2.2 *Concentric-Ring Aerial*

We will first consider the case of a ring in which all the aerial currents are in phase, but there is no central aerial. The method used in Section 2.1 can be applied, putting $n = 0$ in expression (3) and making use of equations (4) and (5).

It follows that the total field strength due to all ring aerials at P is equal to :

$$\frac{E_\theta}{s} \sin(\omega t + \phi) \left\{ s J_0(q \sin\theta) + 2 \sum_{u=1}^{\infty} J_{2u}(q \sin\theta) \sum_{x=1}^{s} \cos(2u\beta) \right\} + \frac{E_\theta}{s} \cos(\omega t + \phi) \left\{ 2 \sum_{u=1}^{\infty} J_{2u-1}(q \sin\theta) \sum_{x=1}^{s} \sin(2u-1)\beta \right\} \quad .. \quad (8)$$

Now $\sum_{x=1}^{s} \cos u\beta = \sum_{x=1}^{s} \cos u\left(\frac{2\pi x}{s} - \alpha\right) =$

$s \cos u\alpha$ or 0,

according as u is or is not an integral multiple of s.

Also, $\sum_{x=1}^{s} \sin u\beta = \sum_{x=1}^{s} \sin u\left(\frac{2\pi x}{s} - \alpha\right) =$

$- s \sin u\alpha$ or 0,

according as u is or is not an integral multiple of s.

Arranging expression (8) in order of ascending Bessel coefficients, in order to determine the dominant deviation term, we find it necessary to distinguish between odd and even values of s. Considering first the case when s is even, $(2u - 1)$ cannot be an integral multiple of s and (8) therefore reduces to :

$$E_\theta \sin(\omega t + \phi) \{J_0(q \sin\theta) + 2J_s(q \sin\theta) \cos s\alpha + 2J_{2s}(q \sin\theta) \cos 2s\alpha + \ldots\}$$

The first term, $E_\theta \sin(\omega t + \phi) J_0(q \sin\theta)$, is the field strength due to an idealized ring containing an infinite number of aerials. The other terms represent the deviation due to the finite number of aerials ; of these the dominant one is the first, $2J_s(q \sin\theta) \cos s\alpha$, compared with which the others can be neglected. There is, therefore, a fluctuation of field strength having one complete cycle between adjacent aerials, and a maximum value of $\pm 2J_s(q \sin\theta)$. The deviation goes down progressively as s is increased, always remembering that s is assumed even.

In the case of the concentric-ring system, in which a single aerial carrying a current k times the ring current is added at the centre, the maximum fractional deviation becomes :

$$\frac{\pm 2J_s(q \sin\theta)}{\{k + J_0(q \sin\theta)\}} \quad .. \quad .. \quad .. \quad (9)$$

This is the normal practical system, since, as Fig. 2 shows, such an arrangement has antifading properties.

The value of the deviation along the ground is found by putting $\theta = 90°$, this gives :

$$\frac{\pm 2J_s(q)}{\{k + J_0(q)\}} \quad .. \quad .. \quad .. \quad (10)$$

This factor is plotted in Fig. 5 for a range of values of ring radius, and for the values of k corresponding to the vertical-radiation diagrams of Fig. 2. If, for instance, a ± 0.1 deviation of field strength is permissible, for a ring radius of 0.25λ four aerials would be required ; for a ring radius of 0.5λ six aerials are needed.

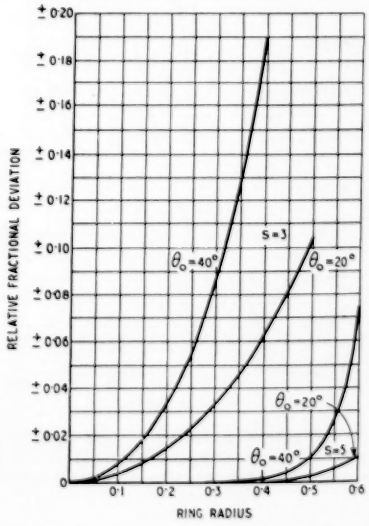

Fig. 6. *Maximum deviation of field strength along ground (s odd) for concentric ring-aerial system ; number of aerials in ring = s.*

For values of θ other than 90°, the deviation is smaller still, as $J_s(q \sin\theta)$ diminishes rapidly with θ ; the simulation of the ideal ring will thus

be even better for small values of θ than when $\theta = 90°$.

The effect of the finite number of aerials at the point in the vertical polar diagram where the radiation for the idealized ring is zero requires special consideration; we will call the angle to the vertical at this point θ_0. It is clear that a value of θ can be found for which the relative field strength is zero for any given value of α; this value, θ'_0, is given by:

$$k + J_0(q \sin \theta'_0) + 2J_s(q \sin \theta'_0) \cos s\alpha = 0.$$

θ'_0 thus varies cyclically with α, there being one complete cycle between adjacent aerials. The maximum and minimum values of θ'_0 are given by the solutions of:

$$k + J_0(q \sin \theta'_0) \pm 2J_s(q \sin \theta'_0) = 0 \quad .. \quad (11)$$

When s is chosen to make the maximum fractional deviation of field strength along the ground small, say not greater than $\pm$ 0.1, and for values of r and θ_0 not exceeding 0.6λ and 40° respectively, the variation of θ_0 is found to be less than $\pm$ 1°; for smaller values of r and θ_0 the variation is correspondingly smaller. The effect of the finite number of aerials in the ring on the vertical polar diagram in the neighbourhood of $\theta = \theta_0$ is therefore negligible.

Summarizing the results of using an even number of aerials in the ring, at any point in space the phase of the field is the same as for an idealized ring, but the amplitude varies with direction. The amplitude deviation is maximum in the ground plane, and has one complete cycle between adjacent aerials. The number of ring aerials being chosen to make this deviation small, say less than $\pm$ 0.1, the effect of the finite number of ring aerials on the vertical polar diagram is also small.

Considering next the case when s is odd, we see that in expression (8) some of the Bessel coefficients multiplying both $\sin(\omega t + \phi)$ and $\cos(\omega t + \phi)$ may have values other than zero, since both $(2u - 1)$ and $2u$ can be integral multiples of s. The first term of the form

$$J_{2u}(q \sin \theta) \sum_{x=1}^{s} \cos 2u\beta$$

which is not zero occurs when $2u = 2s$; the first term of the form

$$J_{(2u-1)}(q \sin \theta) \sum_{x=1}^{s} \sin (2u - 1)\beta$$

which is not zero, on the other hand, occurs when $(2u - 1) = s$.

Proceeding in this way, we find that when s is odd the total field strength at P due to all the ring aerials becomes:

$$E_\theta \sin(\omega t + \phi)\{J_0(q \sin \theta) + 2J_{2s}(q \sin \theta) \cos 2s\alpha + 2J_{4s}(q \sin \theta) \cos 4s\alpha + \ldots\}$$
$$- E_\theta \cos(\omega t + \phi)\{2J_s(q \sin \theta) \sin s\alpha + 2J_{3s}(q \sin \theta) \sin 3s\alpha + \ldots\} \quad .. \quad (12)$$

The Bessel coefficients decrease rapidly as the order increases, so that we need take account of the lowest order coefficient only. The dominant deviation terms is therefore $2J_s(q \sin \theta) \sin s\alpha$, which is in phase quadrature with the main term $J_0(q \sin \theta)$. There will thus be two complete cycles of fluctuation of field strength between adjacent aerials.

If we now include the central aerial, which carries a current k times that of the ring, we obtain the following maximum fractional deviation of field strength from the mean:

$$\pm \frac{\sqrt{\{k + J_0(q \sin \theta)\}^2 + \{2J_s(q \sin \theta)\}^2} - \{k + J_0(q \sin \theta)\}}{2\{k + J_0(q \sin \theta)\}}$$

As s will normally be chosen to make the maximum fractional deviation small, that is

$$\{2J_s(q \sin \theta)\}^2 \ll \{k + J_0(q \sin \theta)\}^2$$

this reduces to:

$$\pm \left\{\frac{J_s(q \sin \theta)}{k + J_0(q \sin \theta)}\right\}^2 \quad .. \quad (13)$$

It is clear that the use of an odd number of aerials, which results in a deviation term in phase quadrature with the main term, has greatly reduced the fluctuations in field strength. Despite this, the next most important term in expression (12), $2J_{2s}(q \sin \theta)$, which is in phase with the main term, can still be neglected since $J_{2s}(z) \ll J_s(z)$ over the range of z in which we are interested.

The maximum deviation of field strength is greatest along the ground, when $\theta = 90°$, and is then:

$$\left\{\frac{J_s(q)}{k + J_0(q)}\right\}^2 \quad .. \quad .. \quad (14)$$

which is plotted in Fig. 6. If we compare this with Fig. 5, the advantage of using an odd number of aerials is evident. For a ring radius containing three aerials, for instance, the fluctuation is approximately one half that when four aerials are used; the superiority of five aerials over six is even more marked.

We must next examine the effect of the finite number of aerials on the vertical polar diagram zero, at $\theta = \theta_0$.

Here $\{k + J_0(q \sin \theta_0)\} = 0$ for the idealized concentric-ring system; for the ring containing a finite number of aerials the field strength at this vertical angle is:

$$- 2E_\theta \cos(\omega t + \phi) J_s(q \sin \theta_0) \sin s\alpha$$

The result of this additional term in the expression for the field strength means that the vertical polar diagram instead of going through a zero at $\theta = \theta_0$ goes through a minimum. The minimum will normally be small, and affect the vertical polar diagram only in the immediate neighbourhood of $\theta = \theta_0$.

For aerials short compared with λ, when $E_\theta = \sin\theta$, the ratio of this minimum field to the ground wave is :

$$\frac{2 \sin\theta_0 \, J_s (q \sin\theta_0) \sin s\alpha}{\{k + J_0 (q)\}}$$

The minimum fluctuates in value, having one complete cycle between aerials, and a maximum of

$$\frac{2 \sin\theta_0 \, J_s (q \sin\theta_0)}{\{k + J_0 (q)\}} \quad .. \quad (15)$$

This maximum value is plotted in Fig. 7, from which we see that when $s = 3$, and θ_0 is as high as 40°, the finite minimum in the vertical polar diagram may rise to high values—sufficiently high to affect the antifading properties of the system

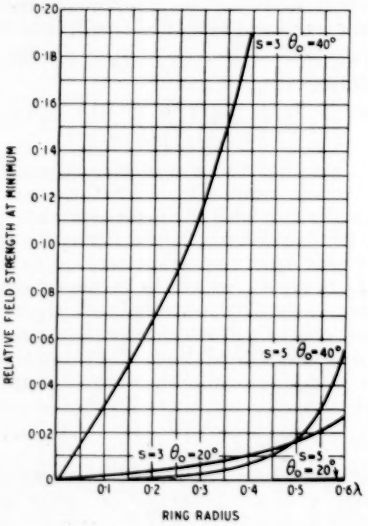

Fig. 7. *Maximum value of field strength at minimum of vertical polar diagram of concentric ring-aerial system.*

appreciably. For smaller values of θ_0, however, three aerials are sufficient. The use of five aerials in the ring never gives rise to appreciable vertical polar-diagram minima, at least over the range of ring radii and θ_0 considered.

Although there are certain cases where three radiators in the ring would be satisfactory, resulting in a small fluctuation in field along the ground, and a small vertical polar-diagram minimum at $\theta = \theta_0$, such a system would not in general be used owing to the restrictions on the values of r and θ_0. A change in operating wavelength may increase the value of r/λ or necessitate an increase in θ_0, either of which may increase the maximum fractional deviation along the ground, and the minimum relative field strength at $\theta = \theta_0$ to undesirably high values.

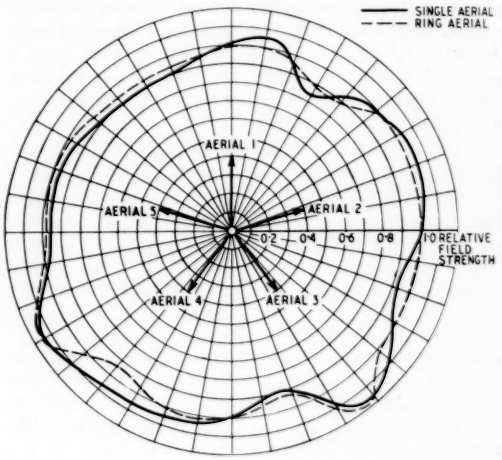

Fig. 8. *Measured horizontal polar diagram of concentric ring-aerial system.*

In general, therefore, the minimum number of aerials in the ring will be four. Consideration of the radiation resistance[1] indicates, however, that a ring radius of the order of 0.35λ is desirable, and in such a case four aerials would lead to a deviation of field strength in the horizontal plane of ± 0.2 when θ_0 is 40°. This deviation may be considered too great, in which case there is a great advantage in using an odd number of ring aerials, and five would normally be chosen.

3. Measurements of a Practical Case

The results of some measurements in one practical case will next be described, in order to show to what extent the theoretical results of Section 2 have been experimentally confirmed. Any attempt to compare the theory with measurements completely would entail an amount of work out of all proportion to the results, and has not been undertaken. Instead, following a theoretical investigation, one particular system was constructed. This was a concentric ring-aerial system, in which the ring had a radius of 0.33λ and contained five aerials, an odd number being chosen to minimize the effect of the finite number. The central aerial was arranged to carry

a current opposite in phase to that of the ring and equal to 0.6 of the total ring current. This corresponded to the vertical-radiation diagram in Fig. 2, having a zero at $\theta = 40°$.

The measurements were made on a wavelength of 342 m, and those concerned with assessing the effect of the finite number of ring aerials were limited to the shape of the horizontal polar diagram. Field-strength measurements were made at a number of 'spot' points at a distance of 5 km from the aerial system. In such circumstances, due to the variation in ground conductivity in different directions, a single aerial does not give a perfectly circular polar diagram, so that the best that could be done was to compare the horizontal polar diagram for the central aerial, without the ring energized, to that of the complete ring system. The results are shown in Fig. 8, in which the individual measurement points and also the position of the ring aerials are indicated. For comparison purposes the mean field strength for each case is made unity.

A study of this figure shows no consistent deviation between the two curves, indicating that the differences are due to measurement errors rather than to the finite number of ring aerials. Measurements repeated at intervals of a few days did in fact indicate variations of the order shown, due possibly to small variations in radiated power, or in the conditions local to the measuring points.

The theoretical deviation in field strength between adjacent aerials would be $\pm 18\%$ for four aerials in the ring, $\pm 0.04\%$ for five aerials and $\pm 0.7\%$ for six aerials. The measurements were sufficiently accurate to show that the deviation was substantially less than the first figure, and there appears no reason to doubt that the theoretical results would be confirmed if high accuracy of measurement could be obtained. The use of five aerials in this particular case was decided on in order to reduce the cyclical deviation to a negligible amount, and this appears to have been achieved.

4. Acknowledgments

The author wishes to thank the Chief Engineer of the British Broadcasting Corporation for permission to publish this paper, and also H. L. Kirke, Head of the B.B.C. Research Department, under whose direction the work was carried out.

REFERENCES

[1] H. Page: "Radiation Resistance of Ring Aerials," *Wireless Engineer* April 1948, Vol. 25, p. 102.

[2] H. Chireix: "Antennes à Rayonnement Zénithal Réduit," *L'Onde Electrique*, July 1936.

V.H.F. VALVES AND CIRCUITS

By M. R. Gavin, M.B.E., M.A., B.Sc., M.I.E.E.

(Communication from the Research Staff of the M.O. Valve Company at the G.E.C. Research Laboratories, Wembley, England)

SUMMARY.—This article discusses some of the aspects of negative-grid valves and their circuits which have not previously been published and indicates certain possible lines of future development.

1. Single-valve Oscillators

THE improvement in performance of negative-grid valves for operation at very high frequencies has been brought about mainly by adapting the valves to suit the circuits in which they operate. In particular, it has been found that there are real advantages in making the valves integral parts of concentric-line circuits with the valve electrodes forming parts of the line[1,2]. An example of this is illustrated in Fig. 1, which shows a triode for operating in a common-anode earthed-anode oscillator. This type of circuit has been used successfully in the decimetre-wave range down to 20 cm.

Considerable success has also been achieved using disc seals for the electrode leads.[2] In this case common-grid circuits are the most suitable, and Fig. 2 shows a common-grid earthed-anode oscillator using a CV90 triode. Valves and circuits of this type have been used at wavelengths down to 10 cm and slightly less.

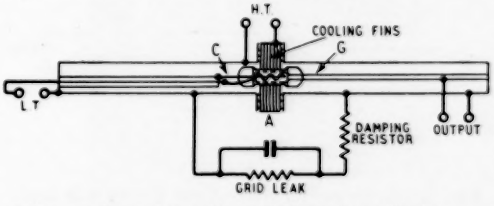

Fig. 1. *Common-anode earthed-anode oscillator.*

When disc-seal valves are used with concentric-line circuits, the diameter of the disc imposes a limit on the maximum frequency which can be obtained in some cases, since the disc acts

MS accepted by the Editor, July 1947

as a series inductance between the electrode and the circuit. In valves with small capacitance this limitation has not proved serious, but it has been found in large valves that a voltage node may occur on or near the disc and the excitation of a

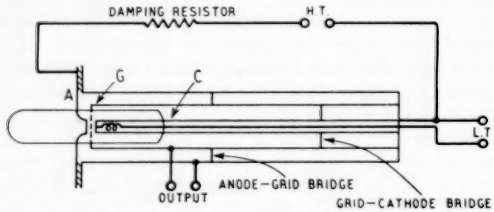

Fig. 2. *Common-grid earthed-anode oscillator using a disc-seal type of triode.*

wave in the associated line circuit may be difficult. This difficulty could probably be eliminated by the use of a space resonator in place of the line, with the disc acting as part of the surface of the resonator. Such a resonator would provide an extremely efficient circuit.

As an alternative to the disc-seal construction an experimental concentric design has been tried as illustrated in Fig. 3. The electrode leads are three concentric copper cylinders with short lengths of glass insulation, and the electrodes are themselves continuations of these cylinders. Apart from the close approach to the ideal valve–circuit combination this design has a number of features which are advantageous. The valve is single-ended and is therefore easy to insert in its circuit. The relatively massive external anode

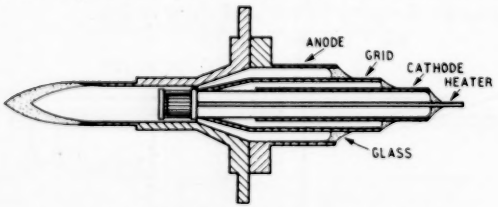

Fig. 3. *Experimental triode Type E1274 with concentric electrodes and leads. The envelope is of copper with glass insulation between the copper tubes.*

makes for easy cooling either naturally or by forced air or water. The grid and cathode assembly is readily visible for inspection and adjustment before the final sealing operation which is made by means of a gold washer between the two flanges on the anode tube and the anode lead. There is a glass pumping stem attached to the anode tube at the end remote from the leads. The oxide-coated cathode has one side of the heater connected internally to the cathode and the other side of the heater is brought out on a wire inside the cathode tube. The grid is mounted directly on its copper tube to provide adequate cooling. Between the cathode and its copper lead there is a short length of thin-walled nichrome tubing to conserve the heating power.

The diagram in Fig. 4 shows the type of circuit that is used. Concentric lines with short-circuited terminations provide variable reactances between the anode and the grid, and the grid and the cathode. The principles of operation of this type of circuit have already been described elsewhere.[2] It will be noted that this arrangement is of the common-grid earthed-anode type; d.c. insulation between the electrodes is provided by means of capacitors built into the circuit at the anode flange and in the grid-cathode shorting

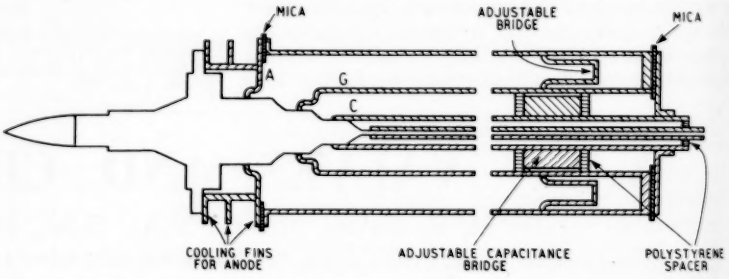

Fig. 4. *Common-grid earthed-anode circuit for use with valve Type E1274.*

bridge. The output may be tapped off the grid-anode line by means of a concentric feeder coupled to the grid tube through a hole in the anode tube.

No definite ratings have been assigned to this valve, but the performance on experimental samples is summarized in Fig. 5. The limiting wavelength is just below 10 cm and for an input of 30 watts the output is about 5 watts at 20 cm and 10 watts at 40 cm.

2. Multi-valve Oscillators

The concentric valve–circuit combination has been used mainly in single-valve oscillators, but the principle may be applied to push-pull circuits by arranging the valves at the opposite ends of a half-wave line. The photograph in Fig. 6 shows such a circuit which was made in 1939 using two valves with the anode and the grid leads in the

form of concentric cylinders.[1] Circuits of this type were subsequently applied to copper-anode valves such as NT93 and NT99, and were used very effectively in naval radar gunnery equip-

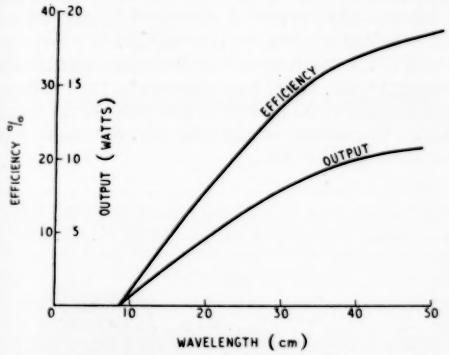

Fig. 5. *Performance of valve Type* E1274 *at a constant input of* 30 *watts.*

ment.[3,6] The cathodes in this circuit are tuned by means of two concentric lines with shorting bridges and the outer conductors of the two discs are both connected together through the surrounding screening box.

This push-pull circuit suffers from certain limitations. With the valves at opposite ends of the circuit change of wavelength is difficult. Again, because of the wide separation of the valves and the open nature of the cathode circuits quite a strong high-frequency field may be set up inside the box, and the outer conductor of the anode–grid line may have currents flowing on it. These factors may affect the operation in a manner difficult to control.

These difficulties may be eliminated by bending the half-wave line into a U-shape, as shown in the diagram of Fig. 7. Now the valves are close together and the anodes may be strapped and earthed. The cathodes may be tuned by means of a single parallel-wire line with a shorting bridge, and the output may be taken from this line. If required the wavelength of the oscillator may be varied by making the parallel section of the anode-grid line of telescopic tubing. This circuit is the push-pull version of the common-anode earthed-anode oscillator.

Where operation at the highest frequencies is not required the concentric anode–grid line may be replaced by a parallel-wire line as shown in Fig. 8 (a) and (b) and in the photograph of Fig. 9. Two CV55 triodes are used in this circuit, and outputs of 20–50 watts may be obtained at wavelengths from 40 to 100 cm. The open-ended grid line shown in Fig. 8 (b) is used at the shorter wavelengths.

Push-pull circuits may also be used with disc seal triodes, and Fig. 10 shows diagrammatically the type of circuit which has been used with CV90 and CV288 triodes. This is an example of a push-pull common-grid earthed-grid oscillator. In most cases the coupling between the anode and the cathode is insufficient to maintain oscillation

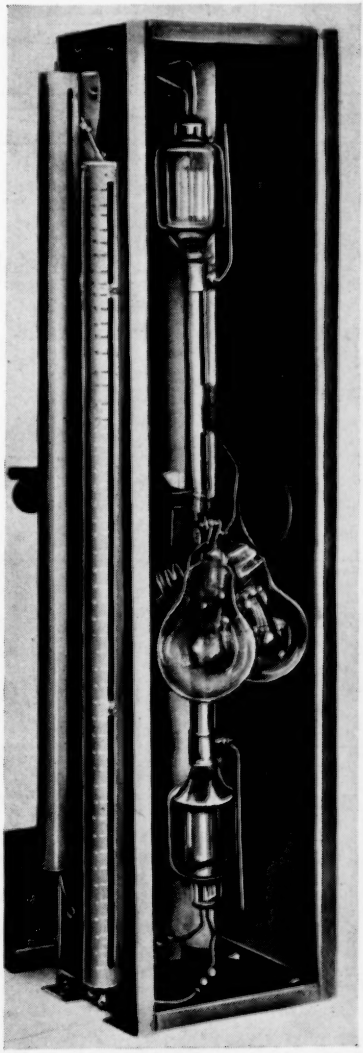

Fig. 6. *Original double-ended concentric oscillator using two experimental triodes with ring seals of eight wires for the anode leads. The wavelength is* 90 *cm and the scale is shown by the engravings on the cathode lines which are* 1 *cm apart.*

and it is essential to connect some capacitance between anode and cathode to provide the necessary feedback.

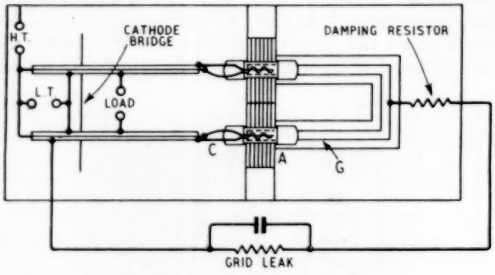

Fig. 7. *Push-pull common-anode earthed-anode oscillator derived from the type of oscillator shown in Fig. 4 by bending the half-wave resonator into U-shape.*

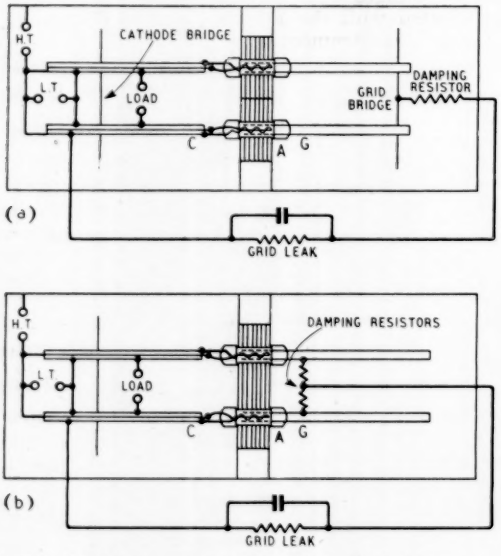

Fig. 8. *Longer-wave versions of the push-pull common-anode earthed-anode oscillator. In (a) both grid and cathode circuits are parallel-wire lines tuned by shorting bridges. In (b) an open-ended grid line is used and the d.c. grid leads are attached at the voltage node. Circuit (b) will operate at a higher frequency than (a).*

Four-valve parallel-push-pull oscillators have been used with CV55 triodes and the photograph of Fig. 11 shows a circuit for operation at 60-cm wavelength with an output of about 100 watts. The four valves have their anodes strapped closely together on a copper block and there are four parallel lines to the grids and to the cathodes. As there are a number of different possible modes of operation of such an arrangement it is necessary to take precautions to ensure operation in the desired mode. In the circuit shown, adjacent valves work in antiphase and it was found that this could be ensured by strapping the diagonally opposed filament leads with a short conductor close to the valves.

In all these oscillators it is desirable to introduce a small series resistance between the shorting bridges and the d.c. feeds to prevent oscillation at a lower frequency where the supply leads form the oscillatory circuit.

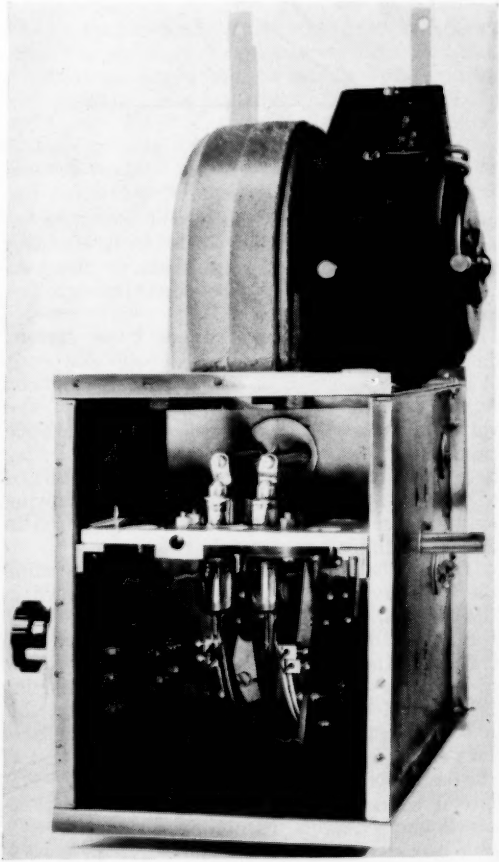

Fig. 9. *Two CV55 triodes in a push-pull common-anode earthed-anode oscillator with parallel-wire lines between the grids and between the cathodes. The cathode line is in the form of an arc to give longer tuning adjustment. The output is taken by means of a loop coupled near the cathode bridge and connected to a co-axial feeder which ultimately comes out at the side of the box. The circuit as shown is for a wavelength of about 60 cm.*

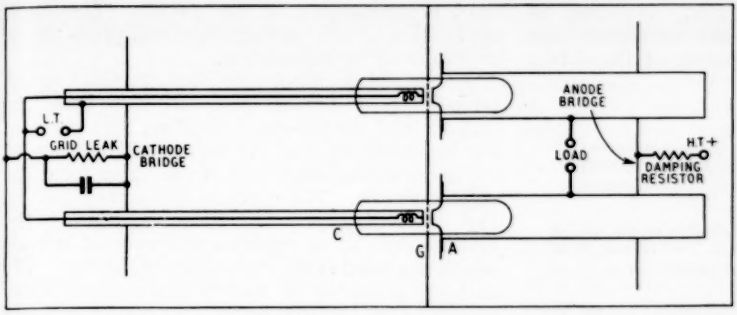

Fig. 10. *Push-pull common-grid earthed-grid oscillator. This circuit may also be used as an amplifier. In this case the input should be supplied by means of a twin feeder to the cathode line. In some cases the cathode line may be omitted and the feeder connected directly to the cathode leads at the valve.*

3. Amplifiers

Practically all of the negative-grid amplifiers for very-high frequencies use the common-grid earthed-grid circuit. The grid, and its continuation outside the valve, act as a screen between the input and output circuits and provided that the anode–cathode capacitance is sufficiently low, stable amplification can be obtained. This arrangement has been used successfully both for receiving[4] and transmitting[2] amplification with valves of the types CV116, CV88, CV273, CV354, CV257 and CV258. All of these valves are of the disc-seal type. The common-anode range of triodes is not suitable for amplification as it is not possible to isolate the input and output circuits.

In the common-grid amplifier the output current flows through the input circuit and as a result there is a large amount of negative feedback. This causes, among other effects, a very low input impedance of the order of the reciprocal of the mutual conductance of the valve. In some cases this low input impedance is beneficial. It means that the tuning of the input circuit is not critical and in some circuits a coaxial feeder can be connected directly between grid and cathode without any matching arrangement. In wide-band circuits the low input impedance is attractive.

Besides these advantages there are, for some applications, certain disadvantages of the common-grid amplifier as compared with the more conventional common-cathode arrangement which is generally used at lower frequencies. In power amplifiers the low input impedance necessitates larger driving power. Some of this power appears in the amplifier

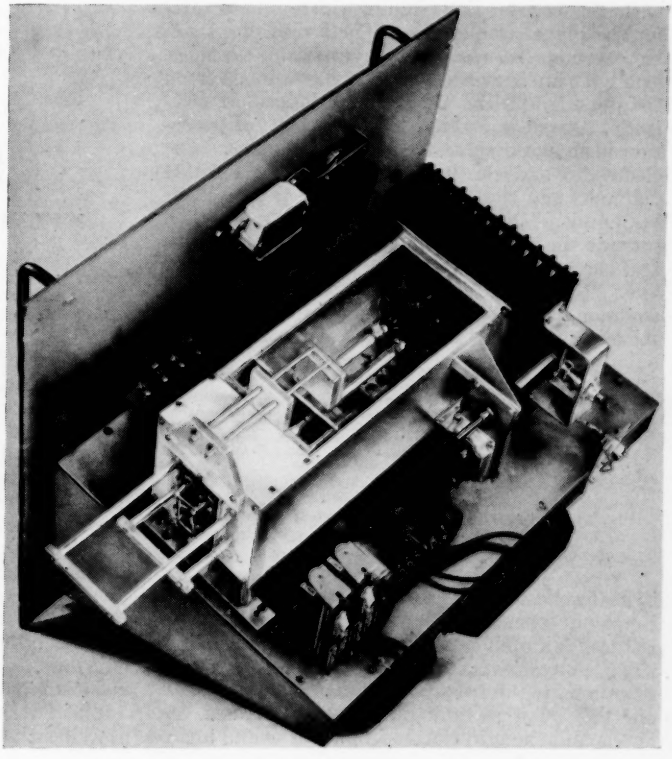

Fig. 11. *A four-valve parallel-push-pull oscillator using CV55 triodes seen from the cathode end. A short length of wire connecting diagonally opposite cathode lines ensures that the corresponding valves operate in phase. The short length of parallel wire feeder at the top takes the output by tapping directly on to one pair of adjacent filament lines. The grid lines, which cannot be seen in the photograph, form a pair of parallel wire lines short-circuited at the end remote from the valves.*

output and is therefore not lost. However, in the case of modulated power amplifiers this effect necessitates the modulation of the driver as well as the final amplifier.

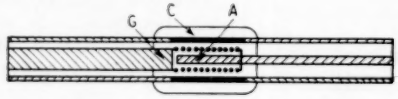

Fig. 12. *Diagrammatic representation of an everted cylindrical triode and its circuit. The cathode is on the outside and the anode is innermost.*

The common-grid amplifier has not proved very successful as a frequency multiplier. Here, large driving voltage is essential for efficient performance and the low input impedance is a real disadvantage.

4. Everted Triodes and Tetrodes[5]

As the common-anode arrangement is unsuited to amplification and the common-grid has disadvantages for certain applications, one is forced to consider the common-cathode which has proved the mainstay of most lower frequency amplifiers. There are difficulties in using common cathodes with the coaxial line circuits which are essential for the higher frequencies. These difficulties can be overcome if the usual cylindrical electrode arrangement is everted so that the cathode is on the outside and the anode is the innermost electrode. A triode arranged for this type of operation is shown diagrammatically in Fig. 12. The electrodes and the leads are all in the form of cylinders and the cathode leads are taken out at both ends. The grid and cathode cylinders then provide the members of the input concentric line and the anode and cathode cylinders the output line. The whole assembly will be seen to form a common-cathode earthed-cathode arrangement. It has already been shown[2] that this arrangement

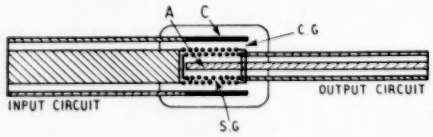

Fig. 13. *An everted cylindrical tetrode and its circuit. The input and output to the two circuits would normally be supplied by means of coxial feeders.*

is not well suited as an oscillator for very-high frequency operation, but it does offer new possibilities for amplification and frequency multiplication. For amplification this arrangement would, of course, require neutralization. This might be effected by a suitable inductance between the anode and the grid electrodes, but it would introduce complications to the circuit. The main application of this arrangement will probably be to frequency multiplication.

For straightforward amplification the everted tetrode offers advantages. In this case the cathode and control-grid cylinders, Fig. 13, form the input circuit and the screen-grid and anode cylinders at the other end of the valve form the output circuit. The cathode and screen are the two earthed electrodes. Fig. 14 shows the arrangement of an experimental everted tetrode which was tried in the early years of the war. The cathode consisted of four boxes symmetrically placed on the circumference of a cylinder with the inner faces oxide-coated and each of the boxes joined to a copper cylinder. The control grid was mounted on the end of a 4-mm tungsten rod

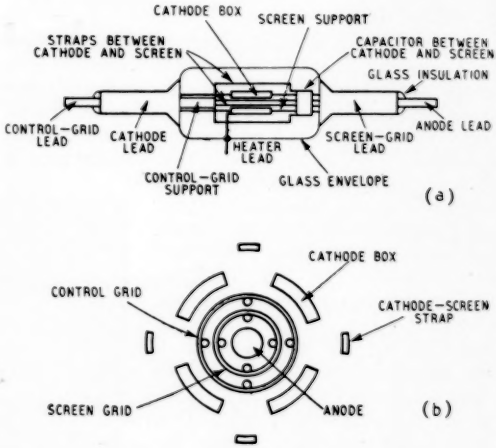

Fig. 14. (*a*) *Experimental everted tetrode (see text).* (*b*) *shows an enlarged cross-sectional view through the electrode system.*

which passed through the copper cylinder with glass insulation. At the other end of the valve the screen-grid was mounted on a similar copper cylinder and the anode consisted of another 4-mm tungsten rod which also formed the anode lead. The cathode and the screen-grid were joined internally by means of four straps passing from the cathode cylinder to a mica capacitor built round the screen-grid cylinder. The two copper cylinders had external feather edges for completing the glass envelope. One end of the heater was joined internally to the cathode and the other end was brought out with a wire through the outer envelope.

This tetrode gave appreciable gain at 50 cm and as far as is known was the first valve to give amplification at this wavelength. The subsequent

introduction of the common-grid triode[4] removed the urgency which was attached to this development but, now that the limitations of the common-grid triode are appreciated it is felt that the everted tetrode may have a part to play in the field of ultra-high frequency amplification, particularly at high power levels and for frequency multiplication. On the score of transit-time effects, tetrodes have an advantage over triodes for class C operation in so far as the screen-grid potential does not drop to a low value at the time of passage of the current pulse.

For radar applications where mean anode dissipations are low and large cathode emission is required everted valves have the advantage that the cathode is the electrode with greatest area.

5. Acknowledgment

In conclusion, the author desires to tender his acknowledgment to the M.O. Valve Co. Ltd., on on whose behalf the work described in this publication was carried out.

REFERENCES

[1] Gavin, M. R. "Triode Oscillators for Ultra-short Wavelengths," *Wireless Engineer*, 1939, Vol. 16, p. 287.

[2] Bell, J., Gavin, M. R., James, E. G., and Warren, G. W. "Triodes for Very Short Waves," *J. Instn elect. Engrs*, 1946, Vol. 93, Part IIIA, No. 5, p. 833.

[3] Ratsey, O. L. "Radar Transmitters," *J. Instn elect. Engrs*, 1946, Vol. 93, Part IIIA, No. 1, p. 245.

[4] Foster, J. "Grounded-grid Amplifier Valves for Very Short Waves." *J. Instn elect. Engrs*, 1946, Vol. 93, Part IIIA, No. 5, p. 868.

[5] Brit. Pat. No. 525,378, Feb. 1939.

[6] England, T. S. "Development of Decimetre-Wave Radar Transmitters for the Royal Air Force." *J. Instn elect. Engrs*, 1946, Vol. 93, Part IIIA, No. 6, p. 1016.

NEW BOOKS

Loran

Edited by J. A. PIERCE, A. A. MCKENZIE and R. H. WOODWARD. (Vol. 4, M.I.T. Radiation Laboratory Series). Pp. 476 + xiv, with 197 illustrations. McGraw-Hill Publishing Co., Ltd., Aldwych, London, W.C.2. Price 36s. (in U.K.).

This volume is one of a wide series in which the team of scientists and engineers of the Radiation Laboratory, M.I.T., have recorded in great detail and from every aspect, almost the whole of their wartime programme of research and development under the control of the National Defense Research Committee.

A notable advance in Radio Aids to Navigation was made during the recent war with the evolution of the hyperbolic lattice system, and it is remarkable that the two earliest examples of systems of this type, Gee and Loran should have been conceived and developed independently and almost simultaneously. (It is acknowledged in this book that the later development of Loran was with the co-operation of Mr. R. J. Dippy, the originator of Gee and his fellow workers.

The book may be fairly described as a book of reference on the whole subject of Loran, for use by the navigator, the cartographer, the physicist and the radio engineer. The first part of the book is concerned with the system, and, comprising five self-contained sections, deals lucidly and comprehensively with the history of the project, what Loran is, and what Loran might eventually come to be. It is introduced by a very useful summary of the various methods of terrestial navigation and the radio systems employing these methods.

Because each section is the work of a different author, or set of authors, there is a tendency for overlapping and repetition, but this only matters if one is reading the book through as a whole.

Probably the most significant feature of the Loran System was the discovery that, under certain circumstances, signals reflected from the ionosphere are of sufficient stability to be used for navigational measurements of a high order of accuracy. Instead of attempting to eliminate the sky-wave component, or accepting the serious limitations imposed by its presence, it was possible to use signals at a range beyond the normal ground-wave cover. The chapter by Mr. J. A. Pierce on propagation deals with this matter in an interesting and thorough fashion. Of particular interest, is the latter half of the chapter dealing with sky-wave on Low-Frequency Loran, that is to say at 180 kc/s.

As far as Mr. Pierce's previous chapter on future trends is concerned, it is to be hoped that the potential customers will not place their hopes too high for the near future. In particular he talks of hyperbolic surveying using cycle matching l.f. Loran to give accuracies of the order of 10 feet. Recent work in this country suggests that much more is to be learnt about low-frequency ground-wave propagation over heterogeneous terrain before accuracies of this order can be expected. It is admitted in the later chapter, Computation of Tables and Charts, that insufficient data are available to evaluate the effect of propagation velocity over land.

The second part of the book deals with the equipment used in the system. Each major item on the ground stations, aerial, transmitter, timing modulator and so on is dealt with in great detail and with adequate illustrations and circuit diagrams. In most cases there have been several models produced, from the semi-experimental equipment advancing to the present day commercial production. Each is separately described. Similarly the receiving equipment, both for marine and air use is dealt with in a painstaking fashion. As an equipment manual it leaves nothing to be desired, but it makes rather hard reading.

In conclusion may it be said that this book can be recommended thoroughly, not to the person who wants to "learn something about Loran," but to whoever, being familiar with the system, is interested in any or every detail about it. G. J. B.

Reports on Progress in Physics, Vol. XI, 1946-47. Pp. 461. The Physical Society, 1, Lowther Gardens, Prince Consort Road, London, S.W.7. Price (to non-Fellows), 42s.

Among the eighteen papers of this book are a number dealing with subjects closely related to the field of wireless. They are "Ferromagnetism," by Edmund C. Stones, "Developments in the Infra-Red Region of the Spectrum," by G. B. B. M. Sutherland and E. Lee, "The Radio-Frequency Spectroscopy of Gases," by B. Bleaney, "The Mechanism of the Thermionic Emission from Oxide-Coated Cathodes," by H. Friedenstein, S. L. Martin and G. L. Munday, and "Meteoric Ionization and Ionospheric Abnormalities," by A. C. B. Lovell.

PROPAGATION OF RADIO WAVES

Measurements with Oblique Incidence on the Ionosphere

By W. J. G. Beynon,* Ph.D., B.Sc.

(Communication from the National Physical Laboratory)

SUMMARY.—The paper deals with some of the results of a series of oblique-incidence ionosphere experiments. Using pulse technique the maximum-usable frequency of region F_2 has been measured over a distance of transmission of 715 km in a direction approximately north-south. The mean measured value is in excellent agreement with that calculated on a simple theoretical basis from simultaneous normal-incidence equivalent-height measurements made at the two ends of the transmission path. In general, the upper frequency limit of the oblique reflections from near the 100-km level (abnormal region-E echoes) shows no close relationship with the corresponding normal-incidence observations. The mean value of a small number of measurements of the separation between the oblique-penetration frequencies of the two magneto-ionic components is not markedly different from that measured at normal incidence at either end of the transmission path. The mean seasonal variation of maximum-usable frequency factors has been measured and compared with that calculated from normal-incidence data. This paper was originally communicated to the Radio Research Board in 1944.

1. Introduction

PRACTICAL short-wave radio-communication problems involve a study of the behaviour of radio waves incident obliquely on the ionosphere, and much of the recent theoretical work has been directed to methods of relating normal-incidence to oblique-incidence phenomena. The experiments described in this paper were principally concerned with the direct measurement, using pulse technique, of the maximum-usable frequency over a sender-receiver distance of 715 km. This measured value has then been compared with that calculated on a simple theoretical basis from simultaneous normal-incidence observations made at each end of the transmission path. These experiments were conducted during various periods of a year and so give some direct measurements of the seasonal variation of both maximum-usable frequencies and maximum-usable-frequency factors. The observations were mainly concerned with reflections from region F_2, but in the course of the experiments some information about oblique reflection from the abnormal region E also became available.

2. Previous Similar Experiments

Experiments similar to those described here have previously been conducted by Farmer and Ratcliffe[1], and by Farmer, Childs and Cowie[2]. The initial experiments of Farmer and Ratcliffe were of very limited accuracy, since normal-incidence ionospheric data were only available at one end of the transmission path. The results of these workers were superseded by the later observations of Farmer, Childs and Cowie. These latter experiments were conducted between Edinburgh and Cambridge, a distance of 464 km in a direction roughly north-south. The observations were made in the period May to August 1937, and due presumably to the limitation of sender power, most of the experiments were conducted at night, at which time the ionospheric absorption of the signal would be a minimum. The observations consisted of a series of visual measurements of the equivalent paths at a number of closely-spaced frequencies. From the results for a group of 21 observations it was concluded that on the average, for a frequency of the order of 7 Mc/s, the observed oblique-penetration frequency for the ordinary ray fell short of that calculated in a simple manner from normal-incidence data by about 0.5%. For this path, the separation between the penetration frequencies of the ordinary and extraordinary ray components is given by these authors as 0.62 ± 0.013 Mc/s, again for a penetration frequency of about 7 Mc/s.

Pulse experiments at oblique incidence are also described in a paper by Crone and others[3] in which some excellent oblique-incidence ($P't$) records were obtained. From the m.u.f. standpoint, however, these results could only be of very limited quantitative accuracy, since data near the mid-point of the trajectory were not available and the period of each experiment was spread over several hours during which considerable ionospheric changes might take place.

3. Theoretical Considerations

For a short distance of transmission, if the effect of the earth's magnetic field is neglected, then the oblique-transmission paths can be calculated from the normal-incidence equivalent-

MS accepted by the Editor, July 1947

* Now at University College, Swansea.

height observations using the fundamental theorems due to Martyn[4] and to Breit and Tuve[5]. Thus if $P'_{(f,i)}$ be the equivalent path of a frequency f incident on the ionosphere at angle i, then

$$P'_{(f,i)} = \sec i.\ P'_{(f\cos i,o)} \quad .. \quad .. \quad (1)$$

where $P'_{(f\cos i,o)}$ represents the equivalent path of a frequency $f\cos i$ incident normally. Furthermore if D is the distance between sender and receiver

$$D = P'_{(f,i)}.\ \sin i \quad .. \quad .. \quad .. \quad (2)$$

so that

$$D\cot i = P'_{(f\cos i,o)} \quad .. \quad .. \quad .. \quad (3)$$

For any given value of D these equations readily enable the oblique-incidence equivalent path $P'_{(f,i)}$ corresponding to any observed normal-incidence equivalent-path $P'_{(f\cos i,o)}$ to be calculated.

The full-line curves shown in Fig. 1(a) and (b) represent normal-incidence equivalent-height/frequency curves typical of those obtained at summer and winter noon at a latitude of 51½° N.

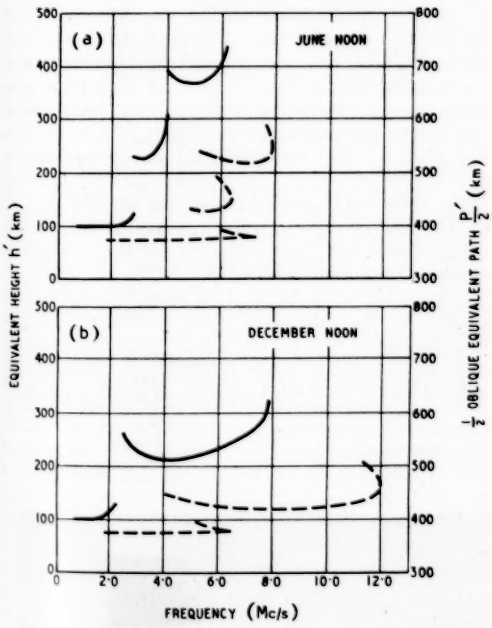

Fig. 1. *Equivalent height/frequency curves for normal (———) and oblique (– – – –) incidence; $D = 715$ km.*

The broken-line curves represent the corresponding oblique-incidence curves for a sender-receiver distance of 715 km calculated from equations (1), (2) and (3). It will be noted that for region F_2 at summer and winter noon we should expect the maximum frequency which could be used at oblique incidence (the m.u.f.) to be respectively about 30% and 50% greater than the normal-incidence critical frequencies. For region E the m.u.f. should be about 2.6 to 2.9 times as large as the normal incidence value.

This analysis is theoretically correct only for small values of D such that the curvature of the earth and the ionosphere can be neglected. For larger values of D the curvature of the earth alone can readily be allowed for by using the chord SBR in place of the arc SAR (Fig. 2)

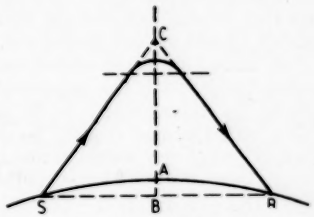

Fig. 2. *Method of allowing for the earth's curvature.*

and increasing the vertical-incidence equivalent height AC by the amount AB. In the present case complete compensation for earth curvature only is thus effected by using a distance of 711 km in place of the true distance 715 km and by increasing the vertical incidence equivalent height measurements by 10 km. Accurate compensation for curvature of the ionosphere can be made only when some specific type of vertical gradient of ionization density in the ionosphere is considered. Now Appleton[6] has shown that with a suitable choice of parameters a parabolic type of gradient will often accurately fit the observed ionospheric conditions. This type of gradient has also been found a useful approximation to actual conditions by Booker and Seaton[7] and by Rydbeck[8]. For a parabolic type of layer of semi-thickness y_m and with lower edge h_0 above the ground, it can readily be deduced from the formulae given by Appleton and Beynon[9, 10] that for that part of the oblique path which lies within the ionosphere the equivalent path of a frequency f incident at angle i is given by

$$P'_{(f,i)} = \int \frac{ds}{\mu} = xy_m \log_e \left(\frac{1 - \dfrac{y_m x^2 \sin^2 i}{R + h_0} + x\cos i}{1 - \dfrac{y_m x^2 \sin^2 i}{R + h_0} - x\cos i} \right) \quad (4)$$

where

$x = f/f^0$

f^0 = ordinary-ray normal-incidence critical frequency

R = radius of the earth.

For the same type of gradient the equivalent

path in the layer of a frequency f_1 incident normally is given by

$$P'_{(f_1,0)} = x_1 y_m \log_e \frac{1 + x_1}{1 - x_1} \quad .. \quad .. \quad (5)$$

where $x_1 = f_1/f^0$.

Calculations for typical ionospheric conditions based on equations (1) and (4) make it clear that for the present distance of transmission (715 km) the effect of ionosphere curvature on values of the equivalent path is very small. The correction to calculated values of the equivalent path necessary on this account should not amount to more than about 25 km at any frequency.

In many of these experiments we were concerned only with the maximum frequency which could be transmitted from sender to receiver. This quantity can readily be determined without constructing the whole of the oblique ($P'f$) curve using one of the several methods now available for the calculation of this quantity[9, 11, 12]. Omitting the effect of the magnetic field of the earth, for this short distance of transmission all methods of calculating the m.u.f. should yield results consistent with those obtained from Martyn's theorem modified slightly, in the manner noted above, to allow for earth curvature.

4. Experimental Procedure

The experiments were made over the transmission path from Burghead (Lat. 57°42′ N, Long. 3°30′ W) to Slough (Lat. 51°30′ N, Long. 0°30′ W) a distance of 715 km, at various times in the period September 1941 to April 1943. Pulse senders of the usual type were installed at both stations, and in most of the experiments signals were radiated from Burghead and received at Slough. In some of the later experiments, however, oblique transmission was operated simultaneously in both directions. The technique employed was similar to that conventionally used for continuous ($h'f$) measurements at normal incidence. The frequency of the sender at Burghead was slowly varied from about 3.6 to 14 Mc/s in a series of five stages. Photographic records were obtained at Slough of the obliquely-incident pulse signals. The time for a complete sweep from 3.6 to 14.0 Mc/s including the intervals necessary for coil changes was normally about 20 minutes, but often the more essential parts of the run were completed in a period of 5 minutes. The experiments were considerably facilitated by the fact that the electric-mains supplies at the sending and receiving sites were synchronized so that time-base units locked to the local-mains supplies could almost always be used. The synchronization was not really perfect since a certain amount of slowly varying phase shift was always present, but the locking was quite adequate for the type of experiment. Vertical-incidence photographic $h'f$ records were available at all times at both stations. At Slough, vertical-incidence $h'f$ observations were made immediately prior and subsequent to the oblique run. At Burghead, a photographic observation of the vertical-incidence $h'f$ curve was obtained simultaneously with the oblique transmission. From these vertical-incidence observations it was thus possible to estimate accurately the ionospheric conditions prevailing at each end of the path at the time of the oblique-incidence experiments. The conditions at the mid-point of the trajectory were then interpolated from these two sets of data. The receivers at both stations were accurately calibrated for frequency against a standard crystal-controlled oscillator.

Fig. 3 shows a typical oblique $h'f$ record obtained in the course of these experiments. No ground signal was received but the interpretation and measurement of the records was considerably helped by the fact that an echo of small amplitude

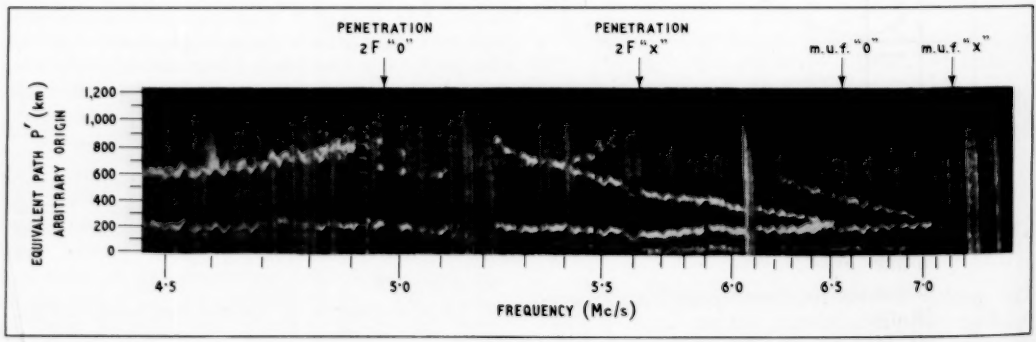

Fig. 3. *Typical oblique incidence ($P'f$) photograph of signals received at Slough from Burghead* (715 *km*); *17th September* 1941, 0703–0713 *G.M.T.*

steadily reflected from near the level of region E was almost always present. The trace of this echo can be seen along the lower edge of Fig. 3. When multiple signals were not present, this echo could often be used as a reference signal from which the intervals of equivalent height could be measured. Fig. 3 shows clearly the high angle of elevation signals (so-called Pedersen rays) which appeared as the m.u.f. was approached.

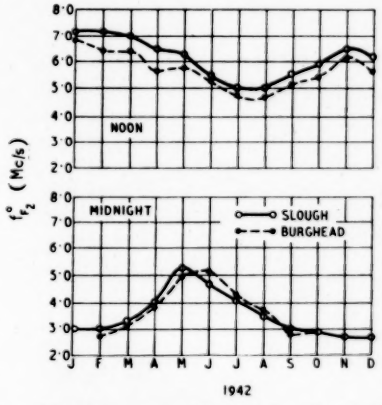

Fig. 4. *Monthly mean critical frequencies at Slough and Burghead.*

The amplitude of this type of signal was comparable with that of the lower-angle ray at frequencies near the m.u.f. but at lower frequencies its amplitude was normally much smaller than that of the lower-angle ray. This Pedersen signal was often not observed until the frequency was quite near the m.u.f. but it was generally possible to distinguish the actual penetration frequency by the sudden large increase in amplitude which occurred as the upper and lower angle of elevation signals coalesced exactly at this frequency. This very marked increase of signal strength to a high maximum at the m.u.f. may be contrasted with the gradual decrease of amplitude which occurs at normal incidence as the critical frequency is reached. Sometimes the extraordinary-ray signal could be observed after the ordinary-ray penetration frequency had been exceeded. Even when it could be recorded the amplitude of this extraordinary component was usually markedly less than that of the ordinary component.

5. Ionosphere Characteristics at Slough and Burghead

One of the objects of these experiments was to compare as accurately as possible, calculated and observed values of the maximum-usable frequency. A calculated estimate of the m.u.f. can be expressed as the product of the normal-incidence critical frequency and a factor (the 'm.u.f. factor') the value of which can be deduced from the normal incidence *h'f* curve. It will assist in forming an estimate of the probable accuracy of such calculated values if we consider briefly some features about the observed vertical-incidence data for Slough and Burghead. Attention throughout has been primarily concentrated upon region F_2, but since the oblique experiments also involved reflections from the abnormal region E, some data on this region are also considered.

(a) *Region F_2 Characteristics.* Curves characteristic of average ionospheric conditions at the two ends of the transmission path are shown in Figs. 4 and 5. These curves give the monthly mean values of region F_2 critical frequency, observed at Slough and Burghead for the year 1942. In general it will be noted that during daylight hours the normal-incidence critical frequencies observed at Slough are a little higher than those observed at Burghead. At noon the mean critical frequency is 6 to 10% higher at Slough than at Burghead, the difference being a little larger during the winter months than during the summer. The night-time values

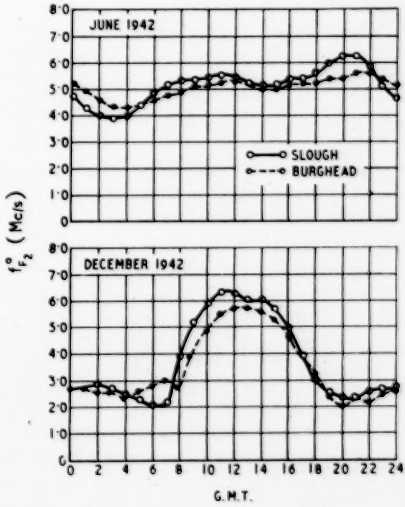

Fig. 5. *Mean diurnal variation of region F_2 critical frequencies Slough and Burghead.*

are not very different at the two stations, but during the summer period because of the longer day at Burghead, the mean night-time critical frequencies at this station are generally slightly larger than are observed at Slough. These

curves are typical monthly mean values, but it must be mentioned that, on individual days, conditions at the two stations could show quite irregular differences.

Two other points may be noted in connection with region F_2 conditions observed at Burghead. Due to the more northerly latitude, conditions at this site were often subject to minor disturbances of the type usually associated with a magnetic storm[13]; i.e., the critical frequency of region F_2 was low and the equivalent height of the region large. In the second place the reflected signals at Burghead were often very spread out in character, so much so that accurate estimation of the critical frequency or of the equivalent height was impossible. It is clear that no accurate comparison between theoretical and experimental maximum-usable frequencies could be effected when conditions at Burghead only were disturbed magnetically or when conditions were such that accurate normal-incidence measurements were not possible.

The detailed shape of the normal incidence *h'f* curve determines the magnitude of the m.u.f. factor and it is interesting to compare m.u.f. factors calculated from simultaneous normal incidence *h'f* curves taken at Slough and at Burghead. From more than 100 comparisons made on ionospherically quiet days it was found that on the average the m.u.f. factors calculated from Slough *h'f* curves differed from the corresponding factors calculated from Burghead data by less than 1%. It must be emphasized that this result refers to the average value of a large number of observations, and in individual cases there may be appreciable divergence from this figure. The mean result does, however, indicate that for these two stations average m.u.f. factors for one station are valid for the other to an accuracy of about 1%.

(b) *Abnormal Region E Reflections.* In addition to the regular differences in region F_2 conditions, marked irregular differences were also noted between the occurrence of abnormal region E reflections at the two stations. As a general rule it can be stated that the incidence of this type of reflection is not closely related at Slough and Burghead. The sporadic nature of this type of reflection makes graphical representation of its occurrence difficult, but from an analysis of a sample of 148 hourly observations taken over two periods of three days in June 1941 and June 1942 it was found that abnormal E echoes were observed on 108 occasions at Slough, but only on 69 occasions at Burghead. The average upper-frequency limit of this type of echo is slightly less at Burghead than at Slough. From a long series of observations at the two stations it can be stated that in general the observation of abnormal region E reflection† at one station was seldom related to its occurrence at the other station. On the other hand, observations of reflection from the level of region E to very high frequencies (this type are usually called intense E echoes) were quite often correlated at the two stations. This observation is consistent with the conclusion that abnormal region E reflections occur from localized areas of ionization, whereas the so-called intense E reflections are characteristic of a widespread area of ionized stratum.

From the foregoing discussion it is possible to form some estimate of the validity of the assumption underlying these oblique-incidence experiments, namely, that conditions near the midpoint of the trajectory could be interpolated from those observed at the two ends. From Figs. 4 and 5 it is clear that for region F_2 under average ionospheric conditions it is unlikely that the estimate of normal-incidence critical frequency near the midpoint of the trajectory will be in error by more than about $\pm$ 0.2 Mc/s. For abnormal region E, however, it is not to be expected that observation of this type of reflection at one or other end of the oblique path can be taken as a reliable indication of the occurrence of such conditions near the mid-point of the trajectory. We shall find that the oblique incidence observations are in general in agreement with these deductions. Thus for region F_2 the mean of a large number of comparisons between theoretical and calculated maximum-usable frequencies is excellent, although individual observations sometimes show quite large discrepancies. For abnormal region E no agreement whatever could be obtained between calculated values based on conditions at Slough and Burghead and the actual observations.

6. Experimental Results

(a) *Measurement of M.U.F. Factors.* A long series of normal-incidence *h'f* curves, has been studied to ascertain the variation to be expected in m.u.f. factors seasonally, diurnally, and with the sunspot cycle. The experimental results described above now enable us to examine the actual measured variations in factors, at least seasonally. In the paper referred to above, it was found that for the latitude of Slough (51½°N) the monthly mean noon factors should increase by about 15 to 20% from summer to winter. The curve showing the seasonal variation in measured mean noon factors deduced from these experiments is shown in Fig. 6. Mean experi-

† Abnormal region E reflection refers to the case in which the upper-frequency limit extends only a short frequency range above the normal region E critical frequency.[14]

mental values are available for only six months in a year, but each point on the curve is the mean of 10 to 30 measurements, so that the average seasonal variation can be fairly accurately assessed. It will be noted that the mean measured factors for a transmission distance of 715 km vary from about 1.26 in summer to about 1.43 in winter representing an increase of some 13% from summer to winter. This figure really refers to a latitude intermediate between that of Slough and Burghead (i.e., to about latitude 54°N) but the seasonal variation noted compares favourably with that previously deduced from the Slough normal-incidence data.

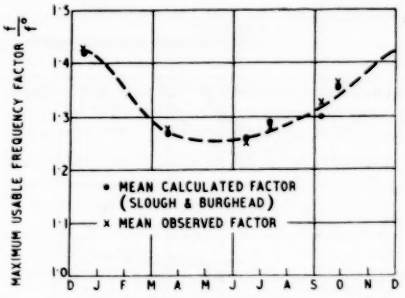

Fig. 6. *Mean seasonal variation of m.u.f. factors; near noon; calculated and observed. D = 715 km.*

Average experimental information for the diurnal variation of m.u.f. factors is rather limited since only in one or two isolated cases were observations continued throughout 24 hours, and there is no certainty that these cases represent the mean diurnal variation.

(b) *Theoretical and Experimental M.U.F. of Region F_2.* We now consider the comparison made between observed values of the m.u.f. and values calculated from the normal-incidence data obtained at the two ends of the path.

Results for a typical day are shown in Fig. 7. This particular set of results contains examples both of the excellent agreement generally observed and also of the considerable disagreement occasionally noted. It will be seen that in general the observed values of the maximum-usable frequency lie between the values calculated from Slough and Burghead data. Thus over the period 0830-0900 G.M.T. on 2nd January, 1943, although there is a difference of more than 2 Mc/s (corresponding to more than 50% difference) between the calculated values, the measured m.u.f. lies within 0.3 Mc/s (or 5%) of the arithmetic mean calculated value. On the same day it will be noted that the curves of calculated values cross over between 10.00 and 11.00 G.M.T. and for a while the value calculated from Burghead data actually exceeds that calculated from Slough data. The measured value is, however, still very close to the arithmetic mean value. During the sunset period from 14.15 G.M.T. onwards we find that all the observed values lie outside the corresponding calculated values and show considerable divergence from the mean calculated values. It must be remembered, however, that over this period ionospheric conditions were changing very rapidly, and it seems very probable that such occasional large divergence can be attributed to the fact that in these circumstances one cannot accurately deduce the ionospheric conditions near the controlling part of the ionosphere. As a general rule it may be said that the best agreement between observed and calculated values was always obtained when conditions at Burghead and at Slough were reasonably steady over a period of a few hours.

From all the experimental results it has been found possible to extract 110 reliable measurements of the maximum-usable frequency of the ordinary-ray component. These 110 values generally refer to daytime observations only, but cover most periods of the year. Of this number, 50 observations show an average discrepancy from the mean calculated values of + 3.8%, 56 show an equal negative discrepancy and 4 show negligible error. It thus appears that positive and negative errors were about

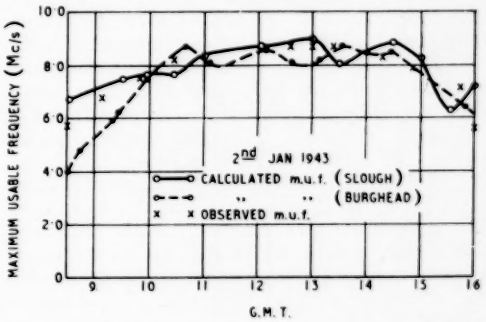

Fig. 7. *Calculated and observed maximum-usable frequencies (ordinary ray component).*

equally probable, the average value in either case being 3.8%. Occasionally (as noted above) the divergence between calculated and observed values reached very high values, but such errors occurred at critical periods of the day when it was to be expected that accurate interpolation for conditions near the midpoint of the trajectory would be very difficult. The divergence of the mean of these 110 measurements amounts only to 0.2%.

The true divergence between the calculated and observed maximum-usable frequencies is unlikely to be as small as this figure suggests, but it seems probable that the agreement is certainly better than 1%. Further comment on this result will be given in Section 7.

(c) *The Maximum-Usable Frequency of the Extraordinary Component.* The effect of the earth's magnetic field on oblique transmission has been analysed by several authors [15, 16], and it is found that the exact calculation depends in a complicated manner on a number of factors such as frequency, strength of the magnetic field at the level of the ionosphere, and direction of the magnetic field relative to the direction of propagation.

In the present experiments special attention was not given to the extraordinary component, but many of the records show both penetration frequencies, and it is of interest to note the measured value of this separation. The mean separations observed at vertical incidence at Slough and Burghead are respectively 0.66 Mc/s and 0.64 Mc/s. The practical measurement of the oblique separation was often upset by the small rapid changes which constantly occur in the value of the oblique penetration frequencies. It was thus necessary to include only the observations taken when conditions were fairly steady. On this account the number of reliable estimates of the oblique separation is somewhat limited. The mean of 16 observations of this separation is 0.66 Mc/s with a probable error of $\pm$ 0.02 Mc/s. The mean value of the ordinary-ray penetration frequency for this set of measurements is 6.0 Mc/s. Thus for this frequency, distance and direction of transmission the frequency separation between the two oblique penetration frequencies is not markedly different from the normal-incidence value. In a later paper it is hoped to present a detailed analysis comparing the measured oblique separation with that calculated theoretically. We may note that Farmer, Childs and Cowie[2] found that with approximately the same direction of transmission the separation at oblique incidence for a sender-receiver distance of 464 km was 0.62 Mc/s.

(d) *Equivalent Paths at Oblique Incidence.* Hitherto we have been concerned with the maximum oblique-incidence penetration frequency, but interest is also attached to an examination of the observations on the oblique equivalent paths at frequencies below the maximum value. If we neglect the influence of the earth's magnetic field then, for a plane ionosphere, equations (1), (2) and (3) enable us to calculate the form of the variation of group path with frequency at oblique incidence. If the effect of ionosphere curvature is included then for the particular case of a parabolic type of gradient the oblique equivalent path can be calculated from equation (4). For the present comparatively short distance of transmission the effect of ionosphere curvature is small and only slight error is introduced by using the much simpler formulae of equations (1)–(3), with an appropriate compensation for the effect of earth curvature only. In these experiments there was no ground signal from sender to receiver, but in most of the oblique records a small reflection from region E was often observed at practically all frequencies

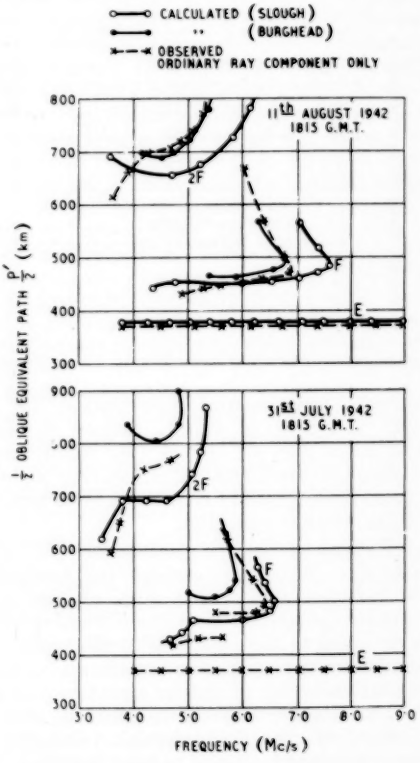

Fig. 8. *Typical oblique incidence (p'f) curves, theoretical and experimental.*

examined. Furthermore from some measurements on lower frequencies at which multiple echo signals were present, it was confirmed that the level of reflection from this region was sufficiently constant to permit of its use as a reference point for the measurement of the intervals of equivalent path. Two typical examples of the comparison which was effected between experi-

mental and theoretical oblique equivalent path frequency curves are shown in Fig. 8. In both cases the experimental traces for region E reflections are shown with a semi-equivalent path of 374 km corresponding to a mean level of reflection of 100 km. These samples are typical of all the results and it will be noted that in general the observed equivalent paths are intermediate between values calculated from Slough and Burghead vertical incidence data. The agreement between the experimental value and the arithmetic mean value of Slough and Burghead is generally within the experimental error of the former, and such divergences as were observed were not greater than would be expected from local variations in ionosphere characteristics. Further reference to these results will be made in Section 7.

(e) *Observations on Abnormal Region E Echoes.* A striking characteristic of the great majority of the oblique records was the fact that an echo of small amplitude reflected from near the level of region E was almost always present. So regular was the occurrence of this echo that one could usually use it as a reference point from which to measure the equivalent paths of the other echoes. An attempt to measure the oblique-penetration frequency of region E was made by Farmer and Ratcliffe[1]. These workers found, however, that this region was irregularly stratified in a horizontal direction, so much so that it was impossible to make any quantitative comparison between theory and experiment. The results of the present work confirm this conclusion, since it appears that, for the sender-receiver distance of 715 km, the highest frequency returned at oblique incidence from about the 100-km level bears little or no relation to the highest frequency returned from this level at normal incidence at either end of the transmission path. In a sample of 50 observations taken in the summer months of June and July it was found that, in almost every case, region E echoes could be observed at frequencies up to at least 10 Mc/s. Often the actual upper limit of frequency was outside the range of the equipment and there were a large number of cases in which the observed value was considerably greater than that expected from the simultaneous vertical-incidence observations. For a sample of 30 observations made in December, at least one-half of these showed marked disagreement with the mean calculated value. It may also be mentioned that in no case was it found possible to identify definitely the Pedersen type of ray which should theoretically appear as the m.u.f. of the normal region was approached. It seems probable that this type of ray is much more attenuated in the case of region E than it is in the case of region F_2 or that the true normal E reflections were always masked by abnormal region E signals. Penetration of the thin abnormal region E stratum would not be expected to show a Pedersen-type ray. On the few occasions when E echoes ceased before the upper-frequency limit had been reached, the cessation was not accompanied by the final sharp maximum in signal strength characteristic of the oblique penetration of region F_2. It is clear that oblique-incidence experiments on echoes returned from near the level of region E, even over this short sender-receiver distance of 715 km, require direct observation of conditions near the midpoint of the trajectory if any success is to be attained. For similar experiments over an east-west path it is possible that data for the two ends would prove more satisfactory than it has in the present instance.

7. Factors Affecting Oblique Propagation

A remarkable result which emerges from these experiments is the extremely close agreement between the mean observed value of the m.u.f. and the mean value calculated in a simple manner from the normal incidence ($h'f$) curves. It may be noted that Farmer, Childs, and Cowie[2] found similar good agreement in their experiments. The mean divergence of about 0.2% deduced from 110 m.u.f. measurements may be compared with a figure of 0.5% obtained by Farmer, Childs and Cowie from a series of 21 measurements. It is doubtful whether the absolute magnitudes of these divergencies are of much significance, but it seems quite safe to state that the systematic divergence between calculated and observed m.u.f. values in both cases is less than 1%. In the present experiments an error of $\pm$ 1% in the m.u.f. corresponds on the average to a divergence of only $\pm$ 0.07 Mc/s. Furthermore, it has been noted that close agreement with simple theory is observed not only for the magnitude of the m.u.f. but also for the intervals of equivalent path (see, for example, Fig. 8). Such close agreement appears all the more remarkable when we remember the simplifications involved in the calculated values. For the ideal case of a plane horizontally-stratified ionosphere in which collisional-frequency effects, the influence of the magnetic field of the earth and the possible influence of a Lorentz 'polarization' term are neglected, the characteristics of oblique transmission can be calculated quite simply, using two fundamental theorems. In the present work and in that of Farmer, Childs and Cowie, the only modification to this simple procedure has been to correct for the curvature of the earth. In practice such ideal conditions do not occur

voltage will cause the capacitance of the specimen to vary cyclicly in phase with the applied a.c., as illustrated in Fig. 3, in which case the material could be developed as a means of obtaining frequency modulation. An answer to this question would also contain information concerning rates of response to changes in d.c. polarization.

The object of the present investigation is to explore these possibilities.

The work is divided into two sections, the first of which is a qualitative demonstration of the cyclic variation of capacitance and the second, an attempt to decide whether the effect of alternating voltages may be quantitatively predicted from the d.c. characteristics.

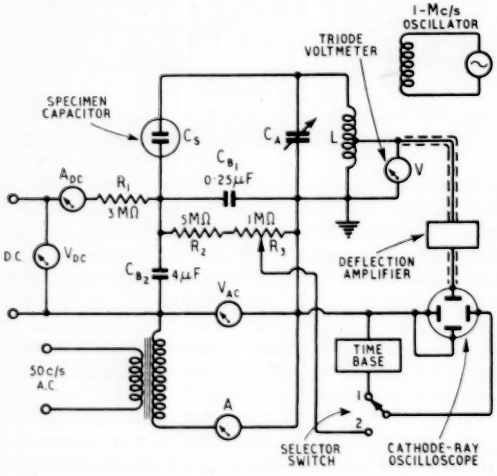

Fig. 4. *Circuit used for qualitative demonstration of cyclic capacitance variation.*

2. Cyclic Capacitance Variation

2.1 *Apparatus used.*

The circuit arrangement of the apparatus used is shown in Fig. 4. A 50-c/s and a unidirectional voltage may be connected in series across the specimen capacitor C_s without their appearing across the tunable air capacitor C_A. C_{B1} is a by-pass capacitor of negligible impedance at the frequency of 1 Mc/s to which the circuit L, C_A, C_s is tuned. The ratio of C_{B1} and C_{B2} is such that only about 5% of the 50-c/s voltage is dropped across C_{B2}.

Unfortunately the oscilloscope available† was not very suitable. The focus obtainable made pattern outlines indeterminate to better than about one millimeter. The deflection amplifiers introduced distortion and it was not possible to calibrate the deflections and thus fix the scale of the traces. It is for this reason that the demonstrations of this section are qualitative only. An oscilloscope with finer focusing, and with accurately linear deflection amplifiers would make possible quantitative studies.

† The work described was carried out in early 1945.

2.2 *Display of Resonance Curve.*

The circuit of Fig. 4 was adjusted in the following manner. With V_{DC} and V_{AC} both zero, the measuring circuit was tuned to resonance with the fixed oscillator frequency of 1 Mc/s by adjusting C_A. The polarizing voltage V_{DC} was then set at 1,800 and the circuit retuned to compensate for the resulting capacitance change of the specimen capacitor. (See Fig. 2). When the time-base was connected to the c.r.o. by placing the selector switch in position 1, a 1-Mc/s wave was displayed on the screen.

With the selector switch placed in position 2 the trace on the c.r.o. became a vertical straight line, but as the 50-c/s voltage V_{AC} was increased from zero this line spread out into a pattern the growth of which, as the voltage was increased to 1,000 volts r.m.s., was recorded by tracing. This is reproduced in Fig. 5, and there related to the d.c. characteristic of Fig. 2. The envelopes are resonance curves on a capacitance base, and asymmetry, due to the excursion of the resultant polarizing voltage beyond the limit of the linear part of the capacitance—voltage characteristic, is clearly seen on the left-hand side of the trace.

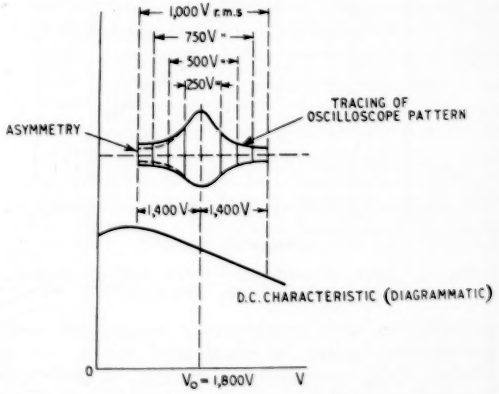

Fig. 5. *Growth of resonance curve pattern as alternating polarizing voltage is increased.*

No looping of the pattern is apparent, which means that no marked 'hysteresis' effect could be present. This conforms to the observation of von Hippel and his colleagues that whereas hysteresis effects exist on the low-temperature

side of the permittivity peak they disappear, or at any rate become relatively very much smaller, at, and on the high-temperature side of, this point, which is the region to which the present investigation relates.

Fig. 6 shows a series of tracings taken as the steady part of the capacitance was varied through the resonant value by adjustment of C_A, for a constant 50-c/s applied voltage of 700 volts r.m.s.

The photographs of Fig. 7 (a) represent a similar series, but in this case with an alternating voltage of 150. These, like the tracings of Fig. 6, were obtained with 50-c/s applied on the X-plates of the c.r.o. For the corresponding series of Fig. 7 (b), on the other hand, a linear time base of 50/3-c/s repetition frequency was applied to the X-plates. It will be seen that when the steady part of the capacitance was adjusted to the centre of the approximately straight-line sides of the resonance curve (traces 1 and 4), the pattern obtained with 50-c/s on the X-plates approximated to a trapezium, and the corresponding pattern with a linear time base shows an amplitude-modulated wave. This is analagous to the well-known method of frequency-modulation to amplitude-modulation conversion using the 'straight' side of a resonance curve. When the steady part of the capacitance was adjusted to the peak of the resonance curve (traces 2 and 3), this peak is swept out in the 50-c/s pattern, and the 50-c/s time-base pattern exhibits a form of frequency doubling of the pattern envelope.

2.3 50-c/s *Repeat Pattern Display.*

For this experiment the circuit of Fig. 4 was adjusted in the following manner :—

With V_{DC} and V_{AC} both zero, the measuring circuit was first tuned to resonance with the fixed oscillator frequency of 1 Mc/s, by adjustment of C_A, and then slightly detuned by *reducing* C_A. With the selector switch in position 2, a straight vertical line was observed on the oscilloscope screen, which line spread out into the pattern shown in Fig. 8 as V_{AC} was increased from zero. This pattern is a graph of the instantaneous voltage across the resonant circuit against the 50-c/s polarizing voltage. The voltage across the resonant circuit is, however, approximately proportional to capacitance change,

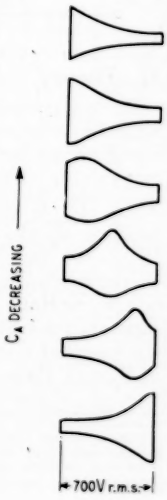

Fig. 6. *Shift of resonance curve pattern with variation of* C_A.

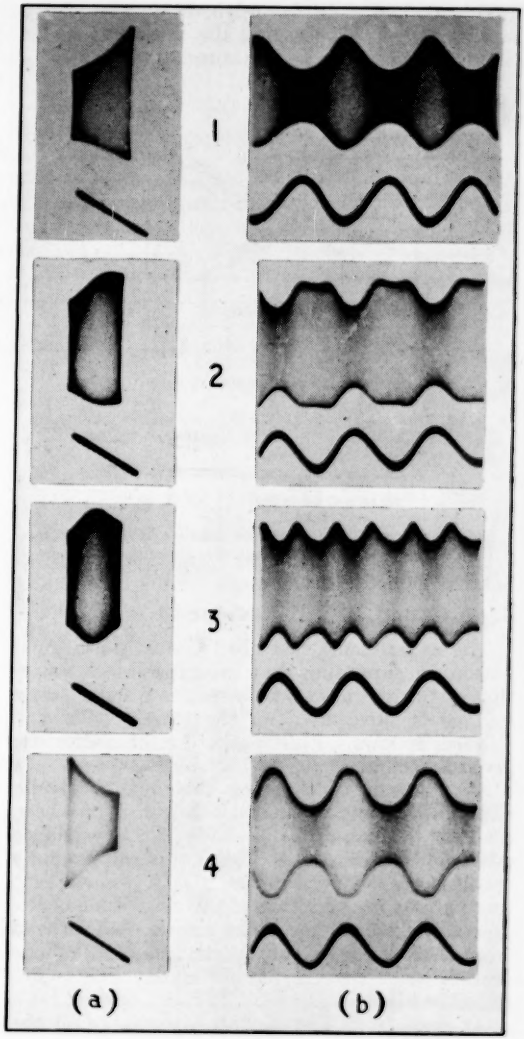

Fig. 7. *50-c/s sine-wave and 50/3-c/s linear time patterns.*

due to the linearity of the side of the resonance curve, so that the pattern of Fig. 8 can also be considered as a graph of capacitance change against 50-c/s polarizing voltage. In other words, the envelope of the pattern is an approximation to the capacitance-voltage characteristic of the material, being modified only by the slight non-linearity of the part of the resonance curve used. The pattern is symmetrical about a vertical axis showing that the variation of capacitance is independent of the sign of the polarizing voltage.

This method of display might be developed as a rapid method of observing the variation of the characteristics with temperature.

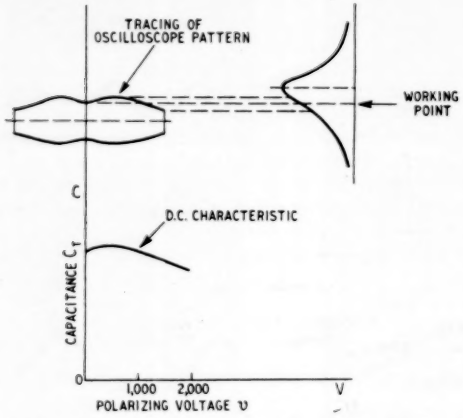

Fig. 8. *Pattern with envelope which approximates to the capacitance/voltage characteristic of the specimen.*

3. A.C. and D.C. Behaviour

The experiments described above afford good reason for supposing that the capacitance variation of the specimen which results when a 50-c/s voltage is superposed on the steady polarizing voltage, follows faithfully the d.c. characteristic given in Fig. 2.

As a means of checking this quantitatively, experimental and mathematical studies have been made of the variations in shape of the resonance curve of the circuit of Fig. 4, (as obtained by reading the valve voltmeter as C_A is varied), associated with variation of the magnitude of the 50-c/s applied voltage. The circuit used differed from that of Fig. 4 only in that the oscilloscope section was removed but for clarity it is reproduced in Fig. 9.

As seen from Fig. 1, the capacitance of the specimen is very sensitive to small changes of temperature, and in order to minimize this possible influence on the results the specimen capacitor was enclosed in a Dewar flask.

3.1 *Experimental procedure.*

With V_{DC} adjusted to, and maintained at, 2,000 volts, V_{dc} was given a succession of values and for each of these values a resonance curve was recorded on the valve voltmeter by variation of the air capacitor C_A. The series of resonance curves is not reproduced as obtained, that is as curves connecting the valve-voltmeter and air-capacitor readings, but four of them corresponding to V_{AC}‡ equal to 0, 195, 400 and 655 volts r.m.s. are given in Fig. 10 as curves connecting V_c/V_m and $\Delta C_A/\Delta C_{A0}$, which variables are defined as follows :—

V_c = valve-voltmeter reading for a setting of C_A displaced by ΔC_A from the resonant value ;

V_m = valve-voltmeter reading at resonance for $V_{AC} = 0$;

ΔC_{A0} = the half-width of the resonance curve for $V_{AC} = 0$ at $1/\sqrt{2}$ of its height.

This conversion of variables is convenient for comparison with theory and has the additional advantage that a calibration of C_A is not required but only evidence of its linearity over the relevant range of ΔC_A.

A further series of experimental results is shown in Fig. 11, obtained by observing the variation of height of the resonance curve with 50-c/s polarizing voltage for a fixed steady polarizing voltage V_{DC} of 2,000 volts.

Fig. 9. *Circuit for resonance curve study.*

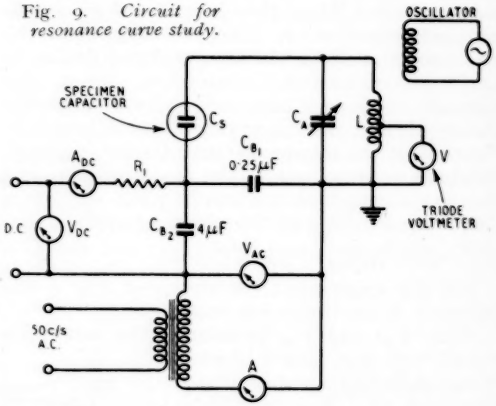

4. Theory

For the purpose of analysis the circuit of Fig. 9 may be reduced to that of Fig. 12, in which $e = E \sin \omega t$ denotes the injected 1-Mc/s voltage, and $C_s = C_o + C \sin pt$ .. .. .. (1) where C_o is the specimen capacitance corresponding to the steady polarizing voltage alone ($V_{AC} = 0$), and C is the peak value of the variation of specimen capacitance due to the superposed 50-c/s voltage $v = \sqrt{2}\, V_{AC} \sin pt$. If the capacitance-voltage characteristic is linear over the range of v, and is of slope K, (=0.0167 in case of Fig. 2), then

$$C = \sqrt{2} K V_{AC} \quad .. \quad .. \quad .. \quad .. \quad (2)$$

‡ These voltage values are the readings of the voltmeter V_{AC} of Fig. 9, less the drop across the by-pass capacitor C_{B_2}, and represent the 50-c/s polarizing voltages applied across C_{B_1} and therefore across the test capacitor Cs.

The total circuit capacitance C_T is therefore, $C_T = C_A + C_o + C \sin pt$

$$= C_F (1 + \lambda \sin pt) \quad .. \quad (3)$$

where $\lambda = \dfrac{C}{C_F} = \dfrac{C}{C_A + C_0}$ .. (4)

and was much less than unity under the experimental conditions previously described.

Referring to Fig. 12, the differential equation governing the instantaneous voltage v_c is,

$$L\frac{d^2}{dt^2}(C_T v_c) + R\frac{d}{dt}(C_T v_c) + v_c = E \sin \omega t,$$

which, by use of (3) may be written

$$LC_F\frac{d^2}{dt^2}\left\{(1 + \lambda \sin pt)\, v_c\right\} + RC_F\frac{d}{dt}\left\{(1 + \lambda \sin pt)v_c\right\}$$

$$+ \frac{1}{(1 + \lambda \sin pt)}\left\{(1 + \lambda \sin pt)v_c\right\} = E \sin \omega t \quad (5)$$

Now since $p/\omega = 1/20{,}000$, $(1 + \lambda \sin pt)$ can be treated as a constant with respect to the variation $\sin \omega t$. Using this approximation, a solution of (5) has been obtained. By finding in the first place the mean value of v_c^2, with respect to the oscillation $\sin \omega t$, and secondly an approximate time average with respect to the oscillation $\sin pt$, the following solution for V_c, corresponding to the valve-voltmeter reading, has been obtained :

$$\left(\frac{V_c}{V_m}\right)^4 = \frac{1}{2x^2} \cdot \frac{\left\{\left(x^2 + y^2 + \dfrac{z^2}{x^2}\right)^2 - 4\dfrac{y^2z^2}{x^2}\right\}^{\frac{1}{2}} + \left\{x^2 - y^2 + \dfrac{z^2}{x^2}\right\}}{\left\{\left(x^2 + y^2 + \dfrac{z^2}{x^2}\right)^2 - 4\dfrac{y^2z^2}{x^2}\right\}} \quad .. \quad .. \quad .. \quad .. \quad (6)$$

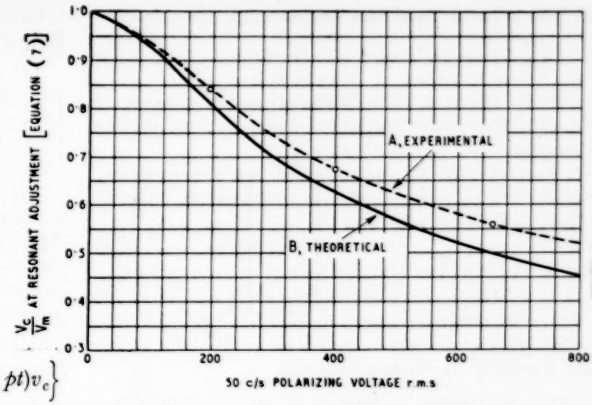

Fig. 11. *Variation of height of resonance curve with 50-c/s polarizing voltage [Equation (7)].*

in which

$x = 1 + \dfrac{1}{Q} \cdot \dfrac{\Delta C_A}{\Delta C_{A0}}$; $y = \dfrac{\Delta C_A}{\Delta C_{A0}}$ and $z = \dfrac{C}{\Delta C_{A0}}$, Q being $1/\omega^2 L \Delta C_{A0}$ and ΔC_A, ΔC_{A0} and C as previously defined. The derivation of (6) is given in the appendix.

When the circuit is adjusted to resonance

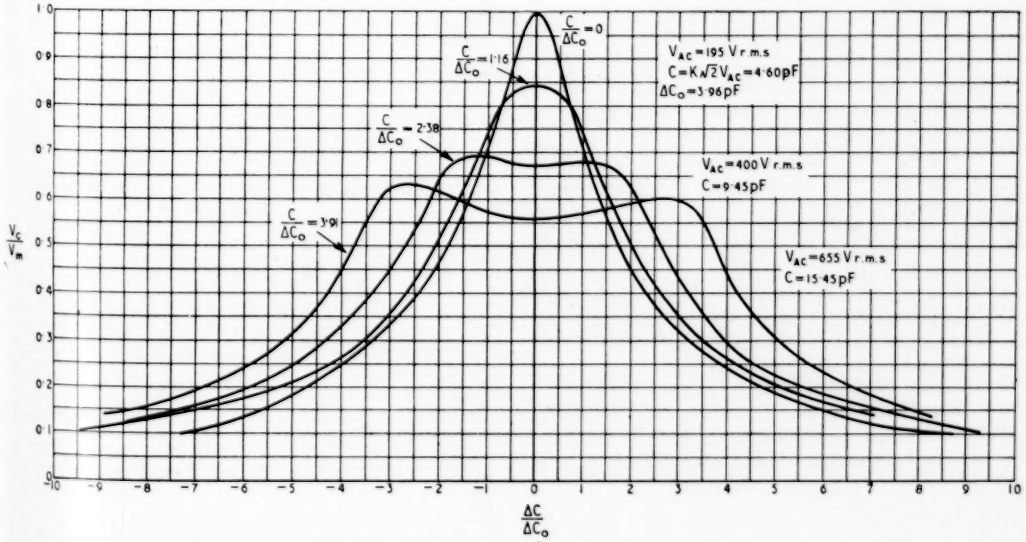

Fig. 10. *Experimental resonance curves.*

curves are typical monthly mean values, but it must be mentioned that, on individual days, conditions at the two stations could show quite irregular differences.

Two other points may be noted in connection with region F_2 conditions observed at Burghead. Due to the more northerly latitude, conditions at this site were often subject to minor disturbances of the type usually associated with a magnetic storm[13]; i.e., the critical frequency of region F_2 was low and the equivalent height of the region large. In the second place the reflected signals at Burghead were often very spread out in character, so much so that accurate estimation of the critical frequency or of the equivalent height was impossible. It is clear that no accurate comparison between theoretical and experimental maximum-usable frequencies could be effected when conditions at Burghead only were disturbed magnetically or when conditions were such that accurate normal-incidence measurements were not possible.

The detailed shape of the normal incidence *h'f* curve determines the magnitude of the m.u.f. factor and it is interesting to compare m.u.f. factors calculated from simultaneous normal incidence *h'f* curves taken at Slough and at Burghead. From more than 100 comparisons made on ionospherically quiet days it was found that on the average the m.u.f. factors calculated from Slough *h'f* curves differed from the corresponding factors calculated from Burghead data by less than 1%. It must be emphasized that this result refers to the average value of a large number of observations, and in individual cases there may be appreciable divergence from this figure. The mean result does, however, indicate that for these two stations average m.u.f. factors for one station are valid for the other to an accuracy of about 1%.

(b) *Abnormal Region E Reflections.* In addition to the regular differences in region F_2 conditions, marked irregular differences were also noted between the occurrence of abnormal region E reflections at the two stations. As a general rule it can be stated that the incidence of this type of reflection is not closely related at Slough and Burghead. The sporadic nature of this type of reflection makes graphical representation of its occurrence difficult, but from an analysis of a sample of 148 hourly observations taken over two periods of three days in June 1941 and June 1942 it was found that abnormal E echoes were observed on 108 occasions at Slough, but only on 69 occasions at Burghead. The average upper-frequency limit of this type of echo is slightly less at Burghead than at Slough. From a long series of observations at the two stations it can be stated that in general the observation of abnormal region E reflection† at one station was seldom related to its occurrence at the other station. On the other hand, observations of reflection from the level of region E to very high frequencies (this type are usually called intense E echoes) were quite often correlated at the two stations. This observation is consistent with the conclusion that abnormal region E reflections occur from localized areas of ionization, whereas the so-called intense E reflections are characteristic of a widespread area of ionized stratum.

From the foregoing discussion it is possible to form some estimate of the validity of the assumption underlying these oblique-incidence experiments, namely, that conditions near the midpoint of the trajectory could be interpolated from those observed at the two ends. From Figs. 4 and 5 it is clear that for region F_2 under average ionospheric conditions it is unlikely that the estimate of normal-incidence critical frequency near the midpoint of the trajectory will be in error by more than about $\pm$ 0.2 Mc/s. For abnormal region E, however, it is not to be expected that observation of this type of reflection at one or other end of the oblique path can be taken as a reliable indication of the occurrence of such conditions near the mid-point of the trajectory. We shall find that the oblique incidence observations are in general in agreement with these deductions. Thus for region F_2 the mean of a large number of comparisons between theoretical and calculated maximum-usable frequencies is excellent, although individual observations sometimes show quite large discrepancies. For abnormal region E no agreement whatever could be obtained between calculated values based on conditions at Slough and Burghead and the actual observations.

6. Experimental Results

(a) *Measurement of M.U.F. Factors.* A long series of normal-incidence *h'f* curves, has been studied to ascertain the variation to be expected in m.u.f. factors seasonally, diurnally, and with the sunspot cycle. The experimental results described above now enable us to examine the actual measured variations in factors, at least seasonally. In the paper referred to above, it was found that for the latitude of Slough (51½°N) the monthly mean noon factors should increase by about 15 to 20% from summer to winter. The curve showing the seasonal variation in measured mean noon factors deduced from these experiments is shown in Fig. 6. Mean experi-

† Abnormal region E reflection refers to the case in which the upper-frequency limit extends only a short frequency range above the normal region E critical frequency.[14]

mental values are available for only six months in a year, but each point on the curve is the mean of 10 to 30 measurements, so that the average seasonal variation can be fairly accurately assessed. It will be noted that the mean measured factors for a transmission distance of 715 km vary from about 1.26 in summer to about 1.43 in winter representing an increase of some 13% from summer to winter. This figure really refers to a latitude intermediate between that of Slough and Burghead (i.e., to about latitude 54°N) but the seasonal variation noted compares favourably with that previously deduced from the Slough normal-incidence data.

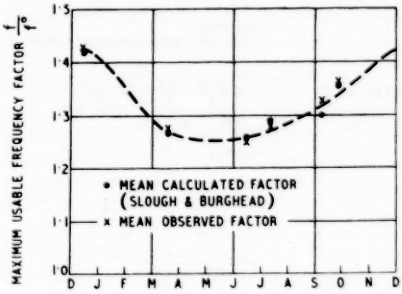

Fig. 6. *Mean seasonal variation of m.u.f. factors ; near noon ; calculated and observed. D = 715 km.*

Average experimental information for the diurnal variation of m.u.f. factors is rather limited since only in one or two isolated cases were observations continued throughout 24 hours, and there is no certainty that these cases represent the mean diurnal variation.

(b) *Theoretical and Experimental M.U.F. of Region F_2.* We now consider the comparison made between observed values of the m.u.f. and values calculated from the normal-incidence data obtained at the two ends of the path.

Results for a typical day are shown in Fig. 7. This particular set of results contains examples both of the excellent agreement generally observed and also of the considerable disagreement occasionally noted. It will be seen that in general the observed values of the maximum-usable frequency lie between the values calculated from Slough and Burghead data. Thus over the period 0830-0900 G.M.T. on 2nd January, 1943, although there is a difference of more than 2 Mc/s (corresponding to more than 50% difference) between the calculated values, the measured m.u.f. lies within 0.3 Mc/s (or 5%) of the arithmetic mean calculated value. On the same day it will be noted that the curves of calculated values cross over between 10.00 and 11.00 G.M.T. and for a while the value calculated from Burghead data actually exceeds that calculated from Slough data. The measured value is, however, still very close to the arithmetic mean value. During the sunset period from 14.15 G.M.T. onwards we find that all the observed values lie outside the corresponding calculated values and show considerable divergence from the mean calculated values. It must be remembered, however, that over this period ionospheric conditions were changing very rapidly, and it seems very probable that such occasional large divergence can be attributed to the fact that in these circumstances one cannot accurately deduce the ionospheric conditions near the controlling part of the ionosphere. As a general rule it may be said that the best agreement between observed and calculated values was always obtained when conditions at Burghead and at Slough were reasonably steady over a period of a few hours.

From all the experimental results it has been found possible to extract 110 reliable measurements of the maximum-usable frequency of the ordinary-ray component. These 110 values generally refer to daytime observations only, but cover most periods of the year. Of this number, 50 observations show an average discrepancy from the mean calculated values of + 3.8%, 56 show an equal negative discrepancy and 4 show negligible error. It thus appears that positive and negative errors were about

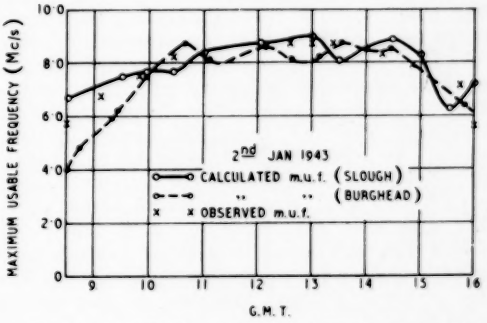

Fig. 7. *Calculated and observed maximum-usable frequencies (ordinary ray component).*

equally probable, the average value in either case being 3.8%. Occasionally (as noted above) the divergence between calculated and observed values reached very high values, but such errors occurred at critical periods of the day when it was to be expected that accurate interpolation for conditions near the midpoint of the trajectory would be very difficult. The divergence of the mean of these 110 measurements amounts only to 0.2%.

The true divergence between the calculated and observed maximum-usable frequencies is unlikely to be as small as this figure suggests, but it seems probable that the agreement is certainly better than 1%. Further comment on this result will be given in Section 7.

(c) *The Maximum-Usable Frequency of the Extraordinary Component.* The effect of the earth's magnetic field on oblique transmission has been analysed by several authors [15, 16], and it is found that the exact calculation depends in a complicated manner on a number of factors such as frequency, strength of the magnetic field at the level of the ionosphere, and direction of the magnetic field relative to the direction of propagation.

In the present experiments special attention was not given to the extraordinary component, but many of the records show both penetration frequencies, and it is of interest to note the measured value of this separation. The mean separations observed at vertical incidence at Slough and Burghead are respectively 0.66 Mc/s and 0.64 Mc/s. The practical measurement of the oblique separation was often upset by the small rapid changes which constantly occur in the value of the oblique penetration frequencies. It was thus necessary to include only the observations taken when conditions were fairly steady. On this account the number of reliable estimates of the oblique separation is somewhat limited. The mean of 16 observations of this separation is 0.66 Mc/s with a probable error of $\pm$ 0.02 Mc/s. The mean value of the ordinary-ray penetration frequency for this set of measurements is 6.0 Mc/s. Thus for this frequency, distance and direction of transmission the frequency separation between the two oblique penetration frequencies is not markedly different from the normal-incidence value. In a later paper it is hoped to present a detailed analysis comparing the measured oblique separation with that calculated theoretically. We may note that Farmer, Childs and Cowie[2] found that with approximately the same direction of transmission the separation at oblique incidence for a sender-receiver distance of 464 km was 0.62 Mc/s.

(d) *Equivalent Paths at Oblique Incidence.* Hitherto we have been concerned with the maximum oblique-incidence penetration frequency, but interest is also attached to an examination of the observations on the oblique equivalent paths at frequencies below the maximum value. If we neglect the influence of the earth's magnetic field then, for a plane ionosphere, equations (1), (2) and (3) enable us to calculate the form of the variation of group path with frequency at oblique incidence. If the effect of ionosphere curvature is included then for the particular case of a parabolic type of gradient the oblique equivalent path can be calculated from equation (4). For the present comparatively short distance of transmission the effect of ionosphere curvature is small and only slight error is introduced by using the much simpler formulae of equations (1)–(3), with an appropriate compensation for the effect of earth curvature only. In these experiments there was no ground signal from sender to receiver, but in most of the oblique records a small reflection from region E was often observed at practically all frequencies

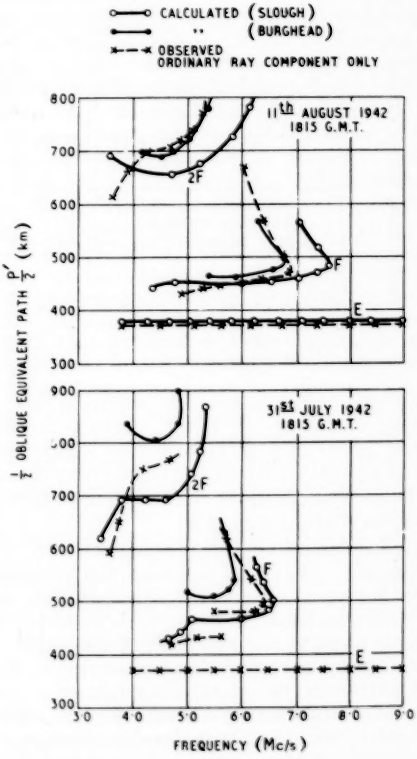

Fig. 8. *Typical oblique incidence (p'f) curves, theoretical and experimental.*

examined. Furthermore from some measurements on lower frequencies at which multiple echo signals were present, it was confirmed that the level of reflection from this region was sufficiently constant to permit of its use as a reference point for the measurement of the intervals of equivalent path. Two typical examples of the comparison which was effected between experi-

mental and theoretical oblique equivalent path frequency curves are shown in Fig. 8. In both cases the experimental traces for region E reflections are shown with a semi-equivalent path of 374 km corresponding to a mean level of reflection of 100 km. These samples are typical of all the results and it will be noted that in general the observed equivalent paths are intermediate between values calculated from Slough and Burghead vertical incidence data. The agreement between the experimental value and the arithmetic mean value of Slough and Burghead is generally within the experimental error of the former, and such divergences as were observed were not greater than would be expected from local variations in ionosphere characteristics. Further reference to these results will be made in Section 7.

(e) *Observations on Abnormal Region E Echoes.* A striking characteristic of the great majority of the oblique records was the fact that an echo of small amplitude reflected from near the level of region E was almost always present. So regular was the occurrence of this echo that one could usually use it as a reference point from which to measure the equivalent paths of the other echoes. An attempt to measure the oblique-penetration frequency of region E was made by Farmer and Ratcliffe[1]. These workers found, however, that this region was irregularly stratified in a horizontal direction, so much so that it was impossible to make any quantitative comparison between theory and experiment. The results of the present work confirm this conclusion, since it appears that, for the sender-receiver distance of 715 km, the highest frequency returned at oblique incidence from about the 100-km level bears little or no relation to the highest frequency returned from this level at normal incidence at either end of the transmission path. In a sample of 50 observations taken in the summer months of June and July it was found that, in almost every case, region E echoes could be observed at frequencies up to at least 10 Mc/s. Often the actual upper limit of frequency was outside the range of the equipment and there were a large number of cases in which the observed value was considerably greater than that expected from the simultaneous vertical-incidence observations. For a sample of 30 observations made in December, at least one-half of these showed marked disagreement with the mean calculated value. It may also be mentioned that in no case was it found possible to identify definitely the Pedersen type of ray which should theoretically appear as the m.u.f. of the normal region was approached. It seems probable that this type of ray is much more attenuated in the case of region E than it is in the case of region F_2 or that the true normal E reflections were always masked by abnormal region E signals. Penetration of the thin abnormal region E stratum would not be expected to show a Pedersen-type ray. On the few occasions when E echoes ceased before the upper-frequency limit had been reached, the cessation was not accompanied by the final sharp maximum in signal strength characteristic of the oblique penetration of region F_2. It is clear that oblique-incidence experiments on echoes returned from near the level of region E, even over this short sender-receiver distance of 715 km, require direct observation of conditions near the midpoint of the trajectory if any success is to be attained. For similar experiments over an east-west path it is possible that data for the two ends would prove more satisfactory than it has in the present instance.

7. Factors Affecting Oblique Propagation

A remarkable result which emerges from these experiments is the extremely close agreement between the mean observed value of the m.u.f. and the mean value calculated in a simple manner from the normal incidence ($h'f$) curves. It may be noted that Farmer, Childs, and Cowie[2] found similar good agreement in their experiments. The mean divergence of about 0.2% deduced from 110 m.u.f. measurements may be compared with a figure of 0.5% obtained by Farmer, Childs and Cowie from a series of 21 measurements. It is doubtful whether the absolute magnitudes of these divergencies are of much significance, but it seems quite safe to state that the systematic divergence between calculated and observed m.u.f. values in both cases is less than 1%. In the present experiments an error of $\pm$ 1% in the m.u.f. corresponds on the average to a divergence of only $\pm$ 0.07 Mc/s. Furthermore, it has been noted that close agreement with simple theory is observed not only for the magnitude of the m.u.f. but also for the intervals of equivalent path (see, for example, Fig. 8). Such close agreement appears all the more remarkable when we remember the simplifications involved in the calculated values. For the ideal case of a plane horizontally-stratified ionosphere in which collisional-frequency effects, the influence of the magnetic field of the earth and the possible influence of a Lorentz 'polarization' term are neglected, the characteristics of oblique transmission can be calculated quite simply, using two fundamental theorems. In the present work and in that of Farmer, Childs and Cowie, the only modification to this simple procedure has been to correct for the curvature of the earth. In practice such ideal conditions do not occur

and propagation should theoretically be influenced by several minor factors. Some of the further corrections which should be included in a complete calculation of the oblique ($h'f$) curve or of the m.u.f. are noted below:—

(a) A small correction should be included to compensate for the curvature of the ionosphere.

(b) In addition to the vertical gradient of ionic density some horizontal gradient is usually also present. The influence of such a horizontal gradient or of a change of layer height would be to produce some asymmetry in the oblique path. As far as a simple reflection from region F_2 alone is concerned it can be deduced from curves given in Figs. 4 and 5 that any horizontal gradient is likely to be very gradual. In practice, however, a more serious source of disturbance might be expected to arise from the deviative influence of regions E and F_1. Such deviation, especially on particular frequencies, might give rise to appreciable distortion of the path. Under such circumstances the controlling part of the ionosphere is not exactly midway between sender and receiver. [See also (c) below.]

(c) The magnetic field of the earth should alter the magnitudes of the equivalent paths at both normal and oblique incidence. Furthermore at oblique incidence the magnetic field should itself give rise to some asymmetry in the trajectory[17].

(d) Finally, it may be noted that the calculated values of the oblique equivalent path will be different depending on whether a Sellmeyer or a Lorentz type of dispersion formula is employed. Theoretical analyses of the effect of using a Lorentz type of formula in place of the usual Sellmeyer formulae have been given by Ratcliffe[17], Smith[18] and Beynon[19].

In practice, some or all of the above factors may be operative simultaneously, and at the present stage an exhaustive theoretical analysis of each of the above factors will not be given. While the effect of any one of these factors may be appreciable, the excellent agreement between simple theory and experiment first noted by Farmer, Childs and Cowie, and confirmed by these extended measurements certainly indicates that for transmission paths up to 700 km at least the net effect of all such factors is usually very small.

8. Acknowledgment

The work described above was carried out as part of the programme of the Radio Research Board to whom it was originally communicated in 1944, and this paper is published by permission of the Department of Scientific and Industrial Research.

REFERENCES

[1] F. T. Farmer and J. A. Ratcliffe, "Wireless Waves reflected from the Ionosphere at Oblique Incidence," *Proc. Phys. Soc.*, 1936, Vol. 48, p. 839.

[2] F. T. Farmer, C. B. Childs, and A. Cowie, "Critical Frequency Measurements of Wireless Waves reflected obliquely from the Ionosphere." *Proc. Phys. Soc.*, 1938, Vol. 50, p. 767.

[3] W. Crone, K. Krüger, G. Goubau and J. Zenneck, "Simultaneous Echo Measurements of Distant Stations." *Hochfrequenztech. u. Elektroakust.*, 1938, Vol. 48, p. 1.

[4] D. F. Martyn, "The Propagation of Medium Radio Waves in the Ionosphere." *Proc. Phys. Soc.*, 1935, Vol. 47, p. 323.

[5] G. Breit and M. A. Tuve, "Test of the Existence of the Conducting Layer." *Phys. Rev.*, 1926, Vol. 28, p. 554.

[6] E. V. Appleton, "Regularities and Irregularities in the Ionosphere,I." *Proc. Roy. Soc.*, 1937, Vol. 162, p. 451.

[7] H. G. Booker and S. L. Seaton, "Relation between Actual and Virtual Ionospheric Height." *Phys. Rev.*, 1940, Vol. 57, p. 87.

[8] O. Rydbeck, "The Propagation of Electromagnetic Waves in an Ionised Medium." *Phil. Mag.*, 1940, Vol. 30, p. 282.

[9] E. V. Appleton and W. J. G. Beynon, "The Application of Ionospheric Data to Radio Communication Problems." Pt. I. *Proc. Phys. Soc.*, 1940, Vol. 52, p. 518.

[10] E. V. Appleton and W. J. G. Beynon, Ditto, Pt. II. *Proc. Phys. Soc.*- 1947, Vol. 59, p. 58.

[11] N. Smith, "Application of Vertical Incidence Ionospheric Measure, ments to Oblique Incidence Radio Transmission." *Journ. Res. Nat. Bur. Stds.*, 1938, Vol. 20, p. 683.

[12] G. Millington, "The Relation between Ionospheric Transmission Phenomena at Oblique Incidence and those at Vertical Incidence." *Proc. Phys. Soc.*, 1938, Vol. 50, p. 801.

[13] E. V. Appleton, R. Naismith and L. J. Ingram, "British Radio Observations during the second International Polar Year 1932-33." *Phil. Trans. Roy. Soc., Lond.*, 1937, Vol. 236, p. 191.

[14] E. V. Appleton and R. Naismith, "Normal and Abnormal Region E Ionisation." *Proc. Phys. Soc.*, 1940, Vol. 52, p. 402.

[15] E. V. Appleton, "Wireless Studies of the Ionosphere." *J. Instn elect. Engrs*, 1932, Vol. 71, p. 642.

[16] H. G. Booker, "Propagation of Wave Packets Incident Obliquely upon a Stratified Doubly Refracting Ionosphere." *Phil. Trans. Roy. Soc.*, 1938, Vol. 237, 0. 411.

[17] J. A. Ratcliffe, "The Effect of the Lorentz Polarisation Term in Ionospheric Calculations." *Proc. Phys. Soc.*, 1939, Vol. 51, p. 747.

[18] N. Smith, "Oblique Incidence Transmission and the Lorentz Polarisation Term." *Bur. Stand. J. Res. Wash.*, 1941, Vol. 26, p. 105.

[19] W. J. G. Beynon, "Oblique Radio Transmission in the Ionosphere and the Lorentz Polarisation Term." *Proc. Phys. Soc.*, 1947, Vol. 59, p. 97.

CYCLIC VARIATIONS OF CAPACITANCE

Effect of 50-c/s Voltages on High-Permittivity Ceramics

By W. Reddish, M.Sc.

1. Introduction

THE remarkable dielectric properties of the barium and strontium titanates, $BaTiO_3$, and $SrTiO_3$, and of solid solutions of the two, have been reported by a number of investigators.* These materials exhibit peak permittivity values of several thousands, the temperature at which the peak value occurs depending on the composition. Thus it occurs in barium titanate at about 120°C and at decreasing temperatures with increasing strontium content in the (BaSr) TiO_3 solid-solution series. The variation of

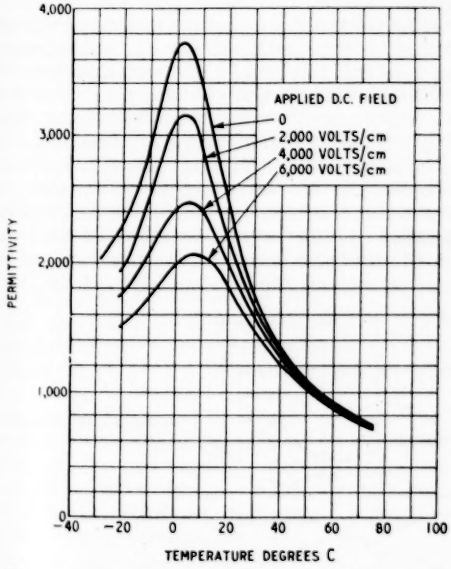

Fig. 1. *Effect of superimposed d.c. field on permittivity of 70:30 (BaSr)TiO_3, measured at 1 Mc/s.*

permittivity with temperature around the peak permittivity point is illustrated for a 70 : 30 (BaSr) TiO_3 composition in Fig. 1, and this figure draws attention to the aspect of behaviour to be considered in this paper, namely the dependence of the permittivity value on applied electric field strength. The permittivity recorded was measured with small alternating field strength (a few volts/cm) at a frequency of 1 Mc/s in the

MS accepted by the Editor, June 1947

* See bibliography

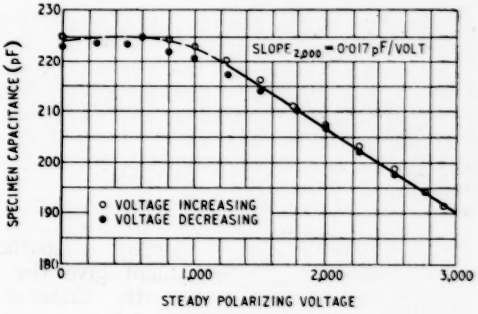

Fig. 2. *D.C. capacitance/voltage characteristic of (70:30) (BaSr) TiO_3 at 1 Mc/s; temperature 21.5°C.*

presence of relatively high unidirectional polarizing fields. The reduction of permittivity with increasing polarizing field strength is most marked near the permittivity peak, and as shown in the capacitance-voltage characteristic of Fig. 2, corresponding to a temperature of 21°C, is a substantially linear one for the specimen in question beyond about 2,000 volts/cm. The slope of the linear part of the curve of Fig. 2 is -0.0167 $\mu\mu$F/volt.

It is evident that there are possible applications of this type of characteristic to automatic-frequency control circuits as an alternative to a reactance valve. The question then arises as to whether a low-frequency alternating voltage, superimposed on a 'biasing' unidirectional

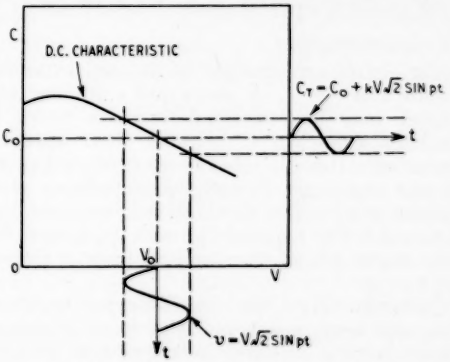

Fig. 3. *Illustrates cyclic capacitance variation using alternating polarizing voltages.*

voltage will cause the capacitance of the specimen to vary cyclicly in phase with the applied a.c., as illustrated in Fig. 3, in which case the material could be developed as a means of obtaining frequency modulation. An answer to this question would also contain information concerning rates of response to changes in d.c. polarization.

The object of the present investigation is to explore these possibilities.

The work is divided into two sections, the first of which is a qualitative demonstration of the cyclic variation of capacitance and the second, an attempt to decide whether the effect of alternating voltages may be quantitatively predicted from the d.c. characteristics.

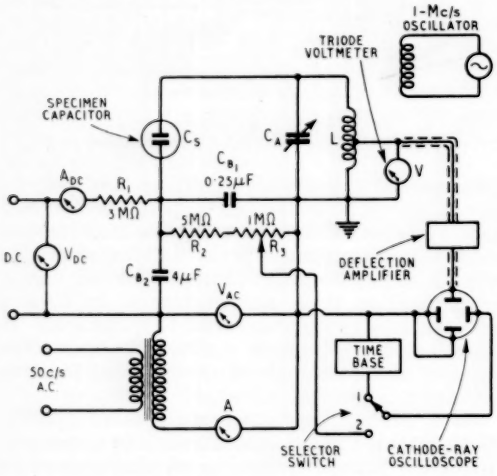

Fig. 4. *Circuit used for qualitative demonstration of cyclic capacitance variation.*

2. Cyclic Capacitance Variation

2.1 *Apparatus used.*

The circuit arrangement of the apparatus used is shown in Fig. 4. A 50-c/s and a unidirectional voltage may be connected in series across the specimen capacitor C_s without their appearing across the tunable air capacitor C_A. C_{B1} is a by-pass capacitor of negligible impedance at the frequency of 1 Mc/s to which the circuit L, C_A, C_s is tuned. The ratio of C_{B1} and C_{B2} is such that only about 5% of the 50-c/s voltage is dropped across C_{B2}.

Unfortunately the oscilloscope available† was not very suitable. The focus obtainable made pattern outlines indeterminate to better than about one millimeter. The deflection amplifiers introduced distortion and it was not possible to calibrate the deflections and thus fix the scale of the traces. It is for this reason that the demonstrations of this section are qualitative only. An oscilloscope with finer focusing, and with accurately linear deflection amplifiers would make possible quantitative studies.

† The work described was carried out in early 1945.

2.2 *Display of Resonance Curve.*

The circuit of Fig. 4 was adjusted in the following manner. With V_{DC} and V_{AC} both zero, the measuring circuit was tuned to resonance with the fixed oscillator frequency of 1 Mc/s by adjusting C_A. The polarizing voltage V_{DC} was then set at 1,800 and the circuit retuned to compensate for the resulting capacitance change of the specimen capacitor. (See Fig. 2). When the time-base was connected to the c.r.o. by placing the selector switch in position 1, a 1-Mc/s wave was displayed on the screen.

With the selector switch placed in position 2 the trace on the c.r.o. became a vertical straight line, but as the 50-c/s voltage V_{AC} was increased from zero this line spread out into a pattern the growth of which, as the voltage was increased to 1,000 volts r.m.s., was recorded by tracing. This is reproduced in Fig. 5, and there related to the d.c. characteristic of Fig. 2. The envelopes are resonance curves on a capacitance base, and asymmetry, due to the excursion of the resultant polarizing voltage beyond the limit of the linear part of the capacitance—voltage characteristic, is clearly seen on the left-hand side of the trace.

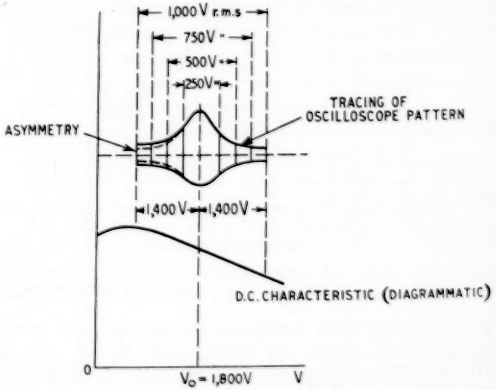

Fig. 5. *Growth of resonance curve pattern as alternating polarizing voltage is increased.*

No looping of the pattern is apparent, which means that no marked 'hysteresis' effect could be present. This conforms to the observation of von Hippel and his colleagues that whereas hysteresis effects exist on the low-temperature

side of the permittivity peak they disappear, or at any rate become relatively very much smaller, at, and on the high-temperature side of, this point, which is the region to which the present investigation relates.

Fig. 6 shows a series of tracings taken as the steady part of the capacitance was varied through the resonant value by adjustment of C_A, for a constant 50-c/s applied voltage of 700 volts r.m.s.

The photographs of Fig. 7 (a) represent a similar series, but in this case with an alternating voltage of 150. These, like the tracings of Fig. 6, were obtained with 50-c/s applied on the X-plates of the c.r.o. For the corresponding series of Fig. 7 (b), on the other hand, a linear time base of 50/3-c/s repetition frequency was applied to the X-plates. It will be seen that when the steady part of the capacitance was adjusted to the centre of the approximately straight-line sides of the resonance curve (traces 1 and 4), the pattern obtained with 50-c/s on the X-plates approximated to a trapezium, and the corresponding pattern with a linear time base shows an amplitude-modulated wave. This is analagous to the well-known method of frequency-modulation to amplitude-modulation conversion using the 'straight' side of a resonance curve. When the steady part of the capacitance was adjusted to the peak of the resonance curve (traces 2 and 3), this peak is swept out in the 50-c/s pattern, and the 50-c/s time-base pattern exhibits a form of frequency doubling of the pattern envelope.

2.3 50-c/s *Repeat Pattern Display.*

For this experiment the circuit of Fig. 4 was adjusted in the following manner :—

With V_{DC} and V_{AC} both zero, the measuring circuit was first tuned to resonance with the fixed oscillator frequency of 1 Mc/s, by adjustment of C_A, and then slightly detuned by *reducing* C_A. With the selector switch in position 2, a straight vertical line was observed on the oscilloscope screen, which line spread out into the pattern shown in Fig. 8 as V_{AC} was increased from zero. This pattern is a graph of the instantaneous voltage across the resonant circuit against the 50-c/s polarizing voltage. The voltage across the resonant circuit is, however, approximately proportional to capacitance change, due to the linearity of the side of the resonance curve, so that the pattern of Fig. 8 can also be considered as a graph of capacitance change against 50-c/s polarizing voltage. In other words, the envelope of the pattern is an approximation to the capacitance-voltage characteristic of the material, being modified only by the slight non-linearity of the part of the resonance curve used. The pattern is symmetrical about a vertical axis showing that the variation of capacitance is independent of the sign of the polarizing voltage.

Fig. 6. *Shift of resonance curve pattern with variation of* C_A.

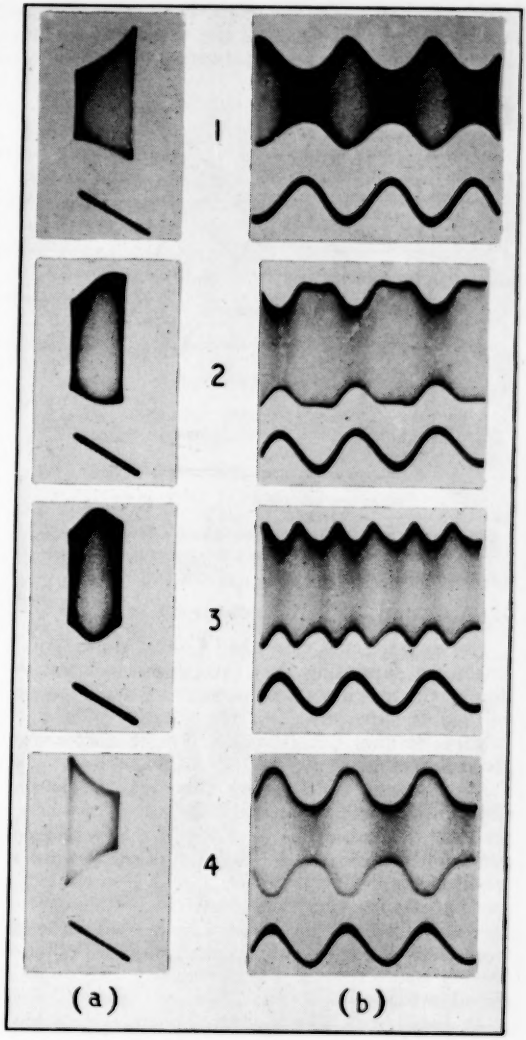

Fig. 7. *50-c/s sine-wave and 50/3-c/s linear time patterns.*

This method of display might be developed as a rapid method of observing the variation of the characteristics with temperature.

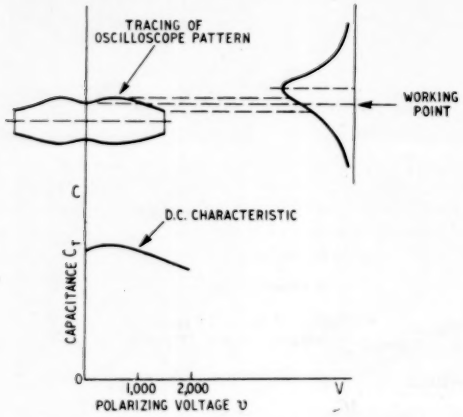

Fig. 8. *Pattern with envelope which approximates to the capacitance/voltage characteristic of the specimen.*

3. A.C. and D.C. Behaviour

The experiments described above afford good reason for supposing that the capacitance variation of the specimen which results when a 50-c/s voltage is superposed on the steady polarizing voltage, follows faithfully the d.c. characteristic given in Fig. 2.

As a means of checking this quantitatively, experimental and mathematical studies have been made of the variations in shape of the resonance curve of the circuit of Fig. 4, (as obtained by reading the valve voltmeter as C_A is varied), associated with variation of the magnitude of the 50-c/s applied voltage. The circuit used differed from that of Fig. 4 only in that the oscilloscope section was removed but for clarity it is reproduced in Fig. 9.

As seen from Fig. 1, the capacitance of the specimen is very sensitive to small changes of temperature, and in order to minimize this possible influence on the results the specimen capacitor was enclosed in a Dewar flask.

3.1 *Experimental procedure.*

With V_{DC} adjusted to, and maintained at, 2,000 volts, V_{dc} was given a succession of values and for each of these values a resonance curve was recorded on the valve voltmeter by variation of the air capacitor C_A. The series of resonance curves is not reproduced as obtained, that is as curves connecting the valve-voltmeter and air-capacitor readings, but four of them corresponding to V_{AC}‡ equal to 0, 195, 400 and 655 volts r.m.s. are given in Fig. 10 as curves connecting V_c/V_m and $\Delta C_A/\Delta C_{A0}$, which variables are defined as follows :—

V_c = valve-voltmeter reading for a setting of C_A displaced by ΔC_A from the resonant value ;

V_m = valve-voltmeter reading at resonance for $V_{AC} = 0$;

ΔC_{A0} = the half-width of the resonance curve for $V_{AC} = 0$ at $1/\sqrt{2}$ of its height.

This conversion of variables is convenient for comparison with theory and has the additional advantage that a calibration of C_A is not required but only evidence of its linearity over the relevant range of ΔC_A.

A further series of experimental results is shown in Fig. 11, obtained by observing the variation of height of the resonance curve with 50-c/s polarizing voltage for a fixed steady polarizing voltage V_{DC} of 2,000 volts.

Fig. 9. *Circuit for resonance curve study.*

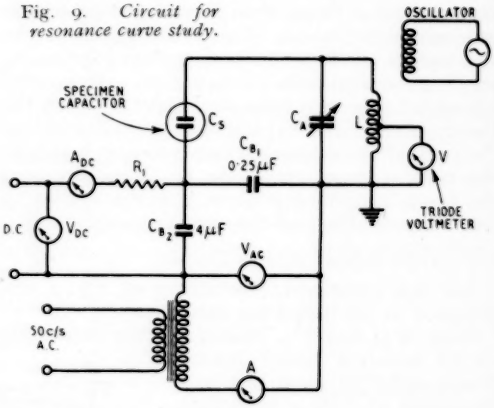

4. Theory

For the purpose of analysis the circuit of Fig. 9 may be reduced to that of Fig. 12, in which $e = E \sin \omega t$ denotes the injected 1-Mc/s voltage, and $C_s = C_o + C \sin pt$ .. .. .. (1) where C_o is the specimen capacitance corresponding to the steady polarizing voltage alone ($V_{AC} = 0$), and C is the peak value of the variation of specimen capacitance due to the superposed 50-c/s voltage $v = \sqrt{2}\, V_{AC} \sin pt$. If the capacitance-voltage characteristic is linear over the range of v, and is of slope K, (=0.0167 in case of Fig. 2), then

$$C = \sqrt{2} K V_{AC} \quad .. \quad .. \quad .. \quad .. \quad (2)$$

‡ These voltage values are the readings of the voltmeter V_{AC} of Fig. 9, less the drop across the by-pass capacitor C_{B_2}, and represent the 50-c/s polarizing voltages applied across C_{B_1} and therefore across the test capacitor C_S.

The total circuit capacitance C_T is therefore, $C_T = C_A + C_o + C \sin pt$

$$= C_F (1 + \lambda \sin pt) \quad .. \quad (3)$$

where $\lambda = \dfrac{C}{C_F} = \dfrac{C}{C_A + C_0}$ .. (4)

and was much less than unity under the experimental conditions previously described.

Referring to Fig. 12, the differential equation governing the instantaneous voltage v_c is,

$$L\frac{d^2}{dt^2}(C_T v_c) + R\frac{d}{dt}(C_T v_c) + v_c = E \sin \omega t,$$

which, by use of (3) may be written

$$LC_F\frac{d^2}{dt^2}\left\{(1 + \lambda \sin pt)\, v_c\right\} + RC_F\frac{d}{dt}\left\{(1 + \lambda \sin pt)v_c\right\}$$

$$+ \frac{1}{(1 + \lambda \sin pt)}\left\{(1 + \lambda \sin pt)\, v_c\right\} = E \sin \omega t \quad (5)$$

Now since $p/\omega = 1/20{,}000$, $(1 + \lambda \sin pt)$ can be treated as a constant with respect to the variation $\sin \omega t$. Using this approximation, a solution of (5) has been obtained. By finding in the first place the mean value of v_c^2, with respect to the oscillation $\sin \omega t$, and secondly an approximate time average with respect to the oscillation $\sin pt$, the following solution for V_c, corresponding to the valve-voltmeter reading, has been obtained :

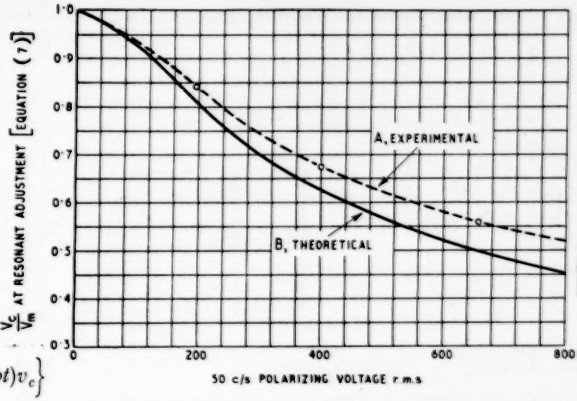

Fig. 11. *Variation of height of resonance curve with 50-c/s polarizing voltage [Equation (7)].*

$$\left(\frac{V_c}{V_m}\right)^4 = \frac{1}{2x^2} \cdot \frac{\left\{\left(x^2 + y^2 + \dfrac{z^2}{x^2}\right)^2 - 4\dfrac{y^2z^2}{x^2}\right\}^{\frac{1}{2}} + \left\{x^2 - y^2 + \dfrac{z^2}{x^2}\right\}}{\left\{\left(x^2 + y^2 + \dfrac{z^2}{x^2}\right)^2 - 4\dfrac{y^2z^2}{x^2}\right\}} \quad .. \quad .. \quad .. \quad .. \quad (6)$$

in which

$x = 1 + \dfrac{1}{Q} \cdot \dfrac{\Delta C_A}{\Delta C_{A0}}$; $y = \dfrac{\Delta C_A}{\Delta C_{A0}}$ and $z = \dfrac{C}{\Delta C_{A0}}$, Q being $1/\omega^2 L \Delta C_{A0}$ and ΔC_A, ΔC_{A0} and C as previously defined. The derivation of (6) is given in the appendix.

When the circuit is adjusted to resonance

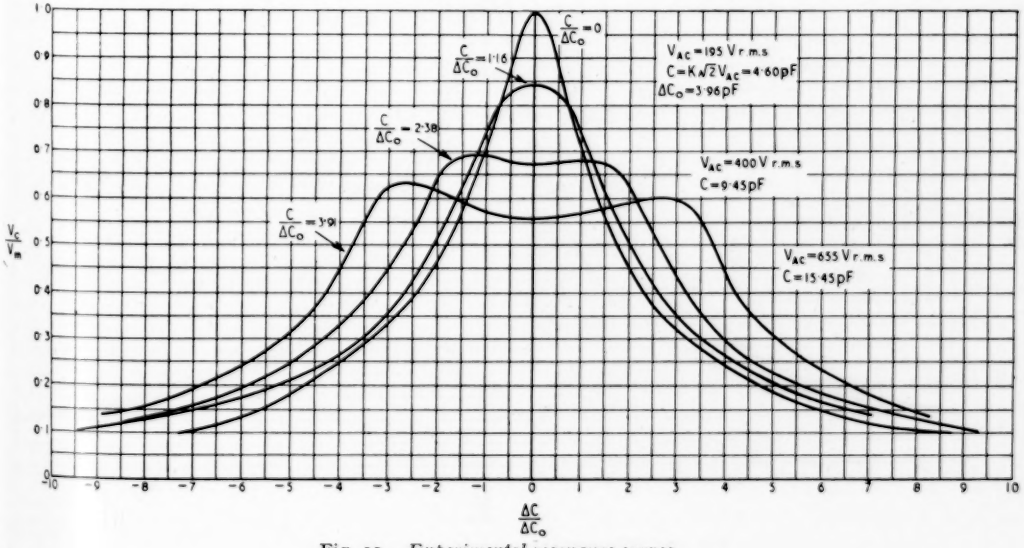

Fig. 10. *Experimental resonance curves.*

$\Delta C_A = 0$, and equation (6) reduces to

$$\left(\frac{V_c}{V_m}\right)^4 = 1\Big/\left[1 + \left(\frac{C}{\Delta C_{A0}}\right)^2\right] \quad .. \quad .. \quad (7)$$

It will be seen that in equation (6), Q appears in a small asymmetry factor only. It is therefore sufficient to calculate V_c/V_m for an average value of Q, if Q is relatively large (100 or more).

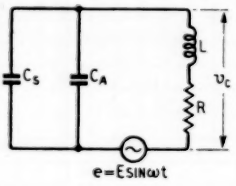

Fig. 12. *Reduced circuit for analysis.*

5. Theory v. Measurements

Fig. 13 shows a family of curves calculated from (6). The curves are of V_c/V_m plotted against $\Delta C_A/\Delta C_{A0}$ with $C/\Delta C_{A0}$ as parameter of the family for $Q = 200$. By choosing $C/\Delta C_{A0}$ as a variable parameter in this way, the amplitude of capacitance swing due to V_{AC} is related to the width of the resonance curve thus helping to give a physical picture of the behaviour. These curves are to be compared with those of Fig. 10. The agreement is good for the lower values of $C/\Delta C_{A0}$ but the results diverge somewhat as $C/\Delta C_{A0}$ increases. The order of the divergence is shown up by Fig. 11 in which the experimental curve A is compared with the curve B, calculated from (7) using $C = K\sqrt{2}$. V_{AC} from (2).

The reasons for the divergence between theory and experiment are not easy to find, but the following are possible :

(1) *Incomplete theory.* Error may arise due to the approximation involved in treating $(1 + \lambda \sin pt)$ as a constant in equation (5), or to neglecting part of the integral in equation (16) in the appendix.

(2) *Incorrect time average* found by the valve voltmeter when the 50-c/s modulation is present. The calibration is shown to be a square law by the very good agreement obtained for $C/\Delta C_{A0} = 0$ between Figs. 10 and 13 ; i.e., for the normal resonance curve.

(3) There may be a small change of slope of the capacitance-voltage characteristic from the d.c. to the a.c. case, due possibly to a small rise of temperature arising from dielectric loss.

The clarification of these points calls for further work which it has not yet been possible to carry out, and it is felt that publication of the data obtained in 1945 should not be further delayed.

6. Conclusions and Remarks

The work shows that cyclic variation of capacitance takes place at 50 cycles per second, and that frequency modulation is possible. The a.c. characteristics can be predicted approximately from d.c. characteristics ; the comparison error is probably less than 20%.

The following points should be considered

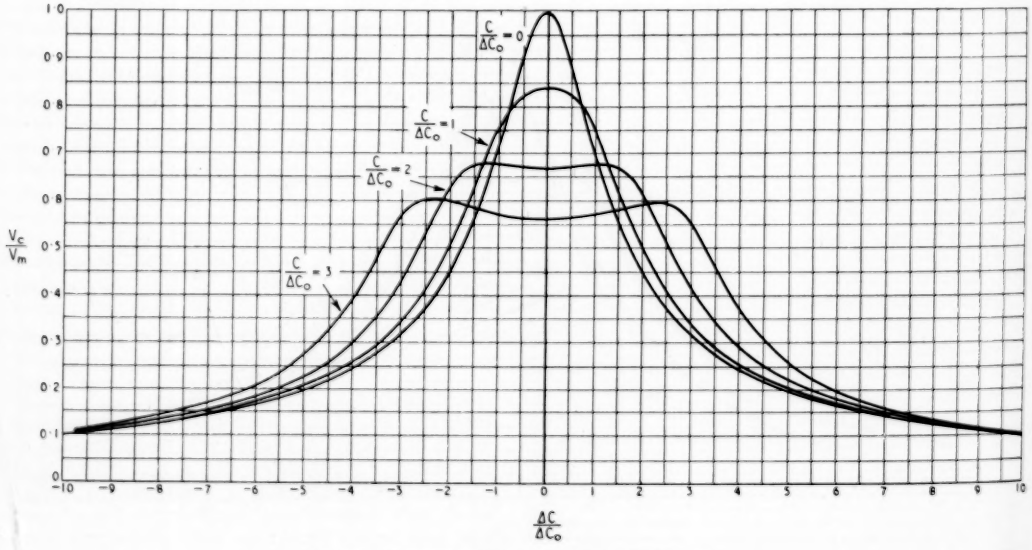

Fig. 13. *Theoretical resonance curves ; $Q = 200$.*

in relation to the application of the ceramics to frequency modulation :

(1) The capacitance values of titanate ceramics are sensitive to temperature changes.

(2) Large modulation voltages have been used in the present work, but this defect could be reduced by developing thin capacitors embedded to prevent surface breakdown.

(3) The results of this report have been obtained with the condition that the modulating field strength is very much larger than the high-frequency strength across the specimen. It is to be expected that the behaviour would be modified if the specimen were to be included in the high radio-frequency voltage circuit of a transmitter. Under such conditions, effects depending on the field strength of the high-frequency voltage would probably appear, as reported by von Hippel and his colleagues.

7. Acknowledgment

The work was carried out in the Electrotechnics Department of Manchester University as part of a programme of extra-mural research for the Ministry of Supply. The author's thanks are due to Professor Willis Jackson and to Messrs. J. Howlett and K. W. Plessner for assistance in this and other allied work.

BIBLIOGRAPHY

Wainer E. and Soloman A. M. Titanium Alloy Mfg. Co., Electrical Reports 8 (1942), 9 and 10 (1943).
Wul, B. *Nature* 1945, Vol. 156, p. 480.
Reddish W. and Jackson W. *Nature*, 1945, Vol. 156, p. 717, and *Trans. of the Faraday Society*, 1946, Vol. XLIIA, 244.
Wainer E., *Trans. Electrochemical Soc.* 1946, Vol. 89, preprint 3.
von Hippel, A., Breckenridge R. G., Chesley F. G., and Tisza L *Industrial and Engineering Chemistry*, 1946, Vol. 38, p. 1097.
Roberts, S. *Physical Review*, 1947, Vol. 71, No. 12, p. 890.

APPENDIX

Solution of equation (5).

If λ is small compared with unity, we may write,

$$1/(1 + \lambda \sin pt) = 1 - \lambda \sin pt$$

when (5) becomes on division by E and LC_F

$$\frac{d^2}{dt^2}\left\{(1 + \lambda \sin pt)\frac{v_C}{E}\right\} + \frac{R}{L}\frac{d}{dt}\left\{(1 + \lambda \sin pt)\frac{v_C}{E}\right\} + \frac{(1 - \lambda \sin pt)}{LC_F}\left\{(1 + \lambda \sin pt)\frac{v_C}{E}\right\} = \sin \omega t \quad .. \quad (8)$$

Treating $(1 + \lambda \sin pt)$ as a constant with respect to the oscillation $\sin \omega t$, the steady-state solution of (8) may be written.

$$(1 + \lambda \sin pt)\frac{v_C}{E} = \frac{[1 - \lambda \sin pt - \omega^2 LC_F] \sin \omega t - \omega R C_F \cos \omega t}{[1 - \lambda \sin pt - \omega^2 LC_F]^2 + \omega^2 R^2 C_F^2}$$

The mean value of $\left(\frac{v_C}{E}\right)^2$ with respect to the oscillation $\sin \omega t$ is, approximately,

$$\overline{\left(\frac{v_C}{E}\right)^2}_\omega = \frac{1}{2} \cdot \frac{1 - 2\lambda \sin pt}{\lambda^2 \sin^2 pt - 2\lambda(1 - \omega^2 LC_F) \sin pt + (1 - \omega^2 LC_F)^2 + \omega^2 R^2 C_F^2} \quad .. \quad .. \quad .. \quad .. \quad (9)$$

If now the resonant value of C_F [equation (3)] is denoted by C_R and C_F/C_R written $(1 + \alpha)$, then

$$(1 - \omega^2 LC_F) = -\alpha \text{ and } \omega^2 R^2 C_F^2 = \left(\frac{1 + \alpha}{Q}\right)^2$$

and (9) becomes

$$\overline{\left(\frac{v_C}{E}\right)^2}_\omega = \frac{1}{2} \cdot \frac{1 - 2\lambda \sin pt}{\lambda^2 \sin^2 pt + 2\alpha\lambda \sin pt + \alpha^2 + \left(\frac{1 + \alpha}{Q}\right)^2} \quad (10)$$

The time average of (10) with respect to the oscillation $\sin pt$ corresponds to the valve-voltmeter reading. The leading term of the integral of (10) can be obtained by neglecting the $2\lambda \sin pt$ term in the numerator, leaving

$$\overline{\left(\frac{v_C}{E}\right)^2} = \frac{1}{2\pi} \cdot \frac{1}{2} \int_0^{2\pi} \frac{1}{\lambda^2 \sin^2 pt + 2\alpha\lambda \sin pt + \alpha^2 + \left(\frac{1 + \alpha}{Q}\right)^2} \cdot dpt \quad .. \quad .. \quad .. \quad (11)$$

The solution of this by resolution into partial fractions may be shown to be,

$$\overline{\left(\frac{v_C}{E}\right)^4} = \frac{Q^4}{8(1 + \alpha)^2} \frac{\{[Q^2(\alpha^2 + \lambda^2) + (1 + \alpha)^2]^2 - 4Q^4\alpha^2\lambda^2\}^{\frac{1}{2}} + Q^2(\lambda^2 - \alpha^2) + (1 + \alpha)^2}{\{Q^2(\alpha^2 + \lambda^2) + (1 + \alpha)^2\}^2 - 4Q^4\alpha^2\lambda^2} \quad .. \quad .. \quad .. \quad (12)$$

In this relation

$$1 + \alpha = \frac{C_F}{C_R} = 1 + \frac{\Delta C_A}{C_R} = 1 + \frac{\Delta C_A}{C_R} \cdot \frac{\Delta C_A}{\Delta C_{A0}} = 1 + \frac{1}{Q} \cdot \frac{\Delta C_A}{\Delta C_{A0}}$$

where ΔC_A and ΔC_{A0} are as defined in Section 3.1 ;

$\alpha = \Delta C_A/C$ and $\lambda = C/C_F$ from equation (4)

On making these substitutions in (12) and finally writing,

$$x = 1 + \frac{1}{Q} \cdot \frac{\Delta C_A}{\Delta C_{A0}} ; \; y = \frac{\Delta C_A}{\Delta C_{A0}} \text{ and } z = \frac{C}{\Delta C_{A0}}$$

the equation becomes

$$\overline{\left(\frac{v_C}{E}\right)^4} = \frac{Q^4}{8x^2} \cdot \frac{\left\{\left[x^2 + y^2 + \frac{z^2}{x^2}\right]^2 - 4\frac{y^2 z^2}{x^2}\right\}^{\frac{1}{2}} + \left\{x^2 - y^2 + \frac{z^2}{x^2}\right\}}{\left\{\left[x^2 + y^2 + \frac{z^2}{x^2}\right]^2 - 4\frac{y^2 z^2}{x^2}\right\}} \quad (13)$$

Now at resonance with $V_{AC} = 0$, $\Delta C_A = 0$ and $C = 0$, so that $x = 1$, $y = z = 0$, and the resonant value V_m of V_C is given by

$$(V_m/E)^2 = Q^4/4$$

Substitution of this in (13) affords the solution stated in equation (6).

CORRESPONDENCE

Letters to the Editor on technical subjects are always welcome. In publishing such communications the Editors do not necessarily endorse any technical or general statements which they may contain.

The Intensity-Distance Law in Radiation

SIR,—I willingly accept the judgment of Drs. Lamont and Saxton on the conditions which are sufficient for the measurement of aerial gain in normal practice, but I still hold to my value of critical-distance parameter for the following reasons :—

(1) The argument from beam cross-section must in general be valid, since one can deduce directivity by comparing the area described by the beam on a sphere of given radius with the total area of the sphere.

(2) Since writing my letter, I have noted two independent publications supporting so large a numerical value of critical distance. Firstly on p. 1469 of the Cutler, King and Kock paper[1] it is stated that for a path difference departing from the mean by not more than $\lambda/16$, " we obtain $r \geqslant 2a^2/\lambda$ [equation (11)] as the required separation between transmitting and receiving aerials. This distance requirement may be too lenient under certain conditions . . . . In Fig. 3, for example, it is seen that at $r = 2a^2/\lambda$ the measured gain is approximately 0.4 db low." Secondly, in a report on German practice in aerial design[2] it is stated (without proof) that " a sufficiently great distance " between transmitting and receiving aerials is $d \gg b^2/2\lambda$ (d = distance, b = aerial width) indicating that $d = b/2\lambda$ is regarded as an inadequate distance.

I agree that it is probably asking too high a degree of accuracy to require $r \gg 2a^2/\lambda$ as a condition of measurement, but I maintain that $r_0 = 2a^2/\lambda$ is a fair representative value for the range beyond which propagation is substantially in accordance with inverse-square law.

D. A. BELL.

British Telecommunications Research Ltd.,
Taplow.

[1] C. C. Cutler, A. P. King and W. E. Kock, *Proc. Inst. Radio Engineers*, Dec. 1947, Vol. 35, p. 1462.
[2] " Dimensioning of Directional Antennas " (according to Dr. Kurt Franz, and reported by A.M. Stevens), F.I.A.T. Final Report No. 610, H.M.S.O., London.

Network Transients

SIR,—An interesting case of network transients occurs when the theory developed by my late brother[1] is applied to the symmetrical constant-resistance type of network. In this instance the extension to multi-section networks is less laborious than for other networks. Two simple examples will serve to illustrate this point. The first is the low-pass filter in Fig. 1 described by Simmonds and Roberts.[2]

Applying the Bisection Theorem and absorbing the generator and load impedances into the branch impedances, we have, using the terminology of the above paper, the following input and output currents for an input step voltage E at $t = 0$,

$$I_{s,r} = \tfrac{1}{2}\left[\frac{E}{R}\left(1 - \frac{1}{2}e^{-tR/L}\right) \pm \frac{E}{2R}e^{-t/CR}\right]_{(t>0)} \quad (1)$$

where $\frac{R}{L} = \frac{1}{CR} = \frac{1}{T}$

or $I_s = E/2R$. . . . . (2

and $I_r = \frac{E}{2R}\left(1 - e^{-t_1}\right)_{(t_1>0)}$ . . . . . (3

where $t_1 = t/T$

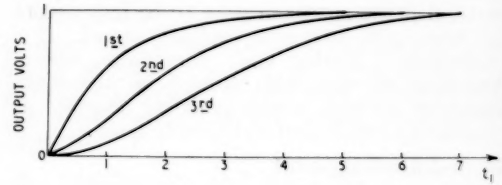

Fig. 2

Equation (2) merely confirms that the network is of the constant-resistance type, and equation (3) shows that the output current is equal to the current that flows when a step of $E/2$ is applied to R and L in series. The voltage applied to a second section replacing the load R would then be $\frac{E}{2}\left(1 - e^{-t_1}\right)$ the first term of which would produce an output similar to equation (3) and the second term an output which may be determined by the method of the Laplace transform.

Using this method it may be deduced that the voltage across the load of the second section is :

$$\frac{E}{2}\left[1 - e^{-t_1} - t_1 \cdot e^{-t_1}\right]_{(t_1>0)} \quad . . \quad . . \quad . . \quad (4)$$

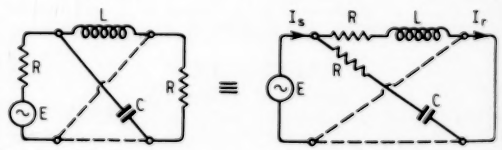

Fig. 3

By a similar process of successive application the voltage appearing across the load of the nth section is :

$$\frac{E}{2}\left[1 - e^{-t_1} - t_1 \cdot e^{-t_1} - \ldots - t_1^{n-1} \cdot \frac{e^{-t_1}}{(n-1)!}\right]_{(t_1>0)} \quad . . \quad . . \quad (5)$$

The transient output voltage after one, two and three sections is shown in Fig. 2.

The second example is the lattice ' all pass ' phase-shift network of Fig. 3. Absorbing the generator and

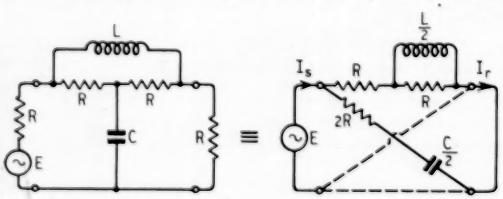

Fig. 1

load impedances as before, we have for the input and output currents of the first section :

$$I_{s,r} = \tfrac{1}{2}\left[\frac{E}{R}\left(1 - e^{-tR/L}\right) \pm e^{-t/CR}\right]_{(t>0)} \quad .. \quad (6)$$

where $\frac{R}{L} = \frac{1}{CR} = \frac{1}{T}$

or $I_s = E/2R$

and $I_r = \frac{E}{2R}\left(1 - 2e^{-t_1}\right)_{(t_1>0)}$ .. .. .. (7)

where $t_1 = t/T$

The voltage input to the second section is then :

$$\frac{E}{2}\left(1 - 2e^{-t_1}\right) \quad (8)$$

The first term produces a similar output to equation (7) from the second section, while the second term produces a voltage output of

$$\frac{E}{2}\left[2e^{-t_1} - 4t_1 . e^{-t_1}\right]_{(t_1>0)} \quad .. \quad .. \quad .. \quad (9)$$

giving a total output voltage from the second section of :

$$\frac{E}{2}\left(1 - 4t_1 . e^{-t_1}\right)_{(t_1>0)} \quad .. \quad .. \quad .. \quad (10)$$

Similarly the voltage output from the third section is

$$\frac{E}{2}\left[1 - 2e^{-t_1} + 4t_1 . e^{-t_1} - 8 . \frac{t_1^2}{2!} . e^{-t_1}\right]_{(t_1>0)} \quad (11)$$

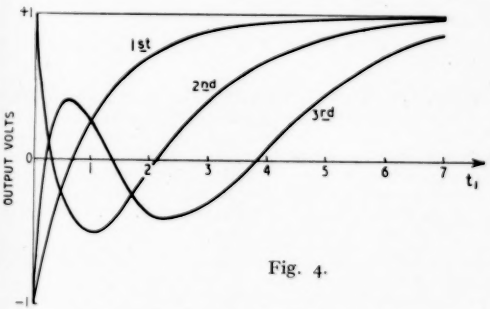

Fig. 4.

The transient output voltage after one, two and three sections is shown in Fig. 4. The severe transient distortion caused by such a network is clearly shown. The general expression for n sections of this network is easily deduced but is rather more cumbersome than equation (5).

E. V. D. GLAZIER.

Barton-on-Sea, Hants.

[1] A. W. Glazier, "Transient Response of Symmetrical 4-Terminal Networks," *Wireless Engineer*, January 1948, p. 11.
[2] F. F. Roberts and J. C. Simmonds, "The Physical Realisability of Networks, with Particular Reference to those of the Probability Function Type." *Phil. Mag.*, November 1944, p. 778.

Standard Terms and Abbreviations

SIR,—Prof. Howe's Editorial and Mr. Jefferson's letter, appearing with mine in your July issue, prompt me to return unexpectedly soon to this subject. Mostly I agree with both, but a few points must be taken up.

First, Mr. Jefferson's typewriter. It is a simple matter, done in an hour without losing the machine, to have some old keys replaced by new. I usually urge that a machine used for my work has some of the unwanted characters, such as ¾ ½ ¼ @ £ ¢ ½ ¼, replaced by useful ones like μ ω Ω + > [ ] $\int$ /. It is then wonderful how much, and how neatly, mathematics can by typed.

An aggravating feature of the standard keyboard is its inability to distinguish between 1 and l.

The prefix giga (G = 10^9, presumably pronounced as in gigantic) seems worthy of adoption in place of kM. My colleagues will witness that I used mμF (*not* kpF) for years before I found salvation in nano (n = 10^{-9}). Dr. Latimer incites me to suggest that if 1 pF is colloquially known as a puff and is somewhat small, then 1 nF might be a nuff.

Prof Howe appears to maintain that only those *combinations* of prefixes and units which have been officially recognized should be abbreviated. Now I find the neper and millineper considerably more convenient than the decineper in practical calculations : am I then to be condemned for ever to writing them in full ? But B.S.560 (1934, p.37) specifically encourages us to combine abbreviations for prefixes and units And we must expect others to adopt our abbreviations ; for instance the gigagramme (Gg) would be a suitable unit for the capacity of ships, and would not limit their cargoes to horseflesh.

Regarding the unit of inductance, mentioned in passing in my previous letter, it seems a pity that when Heaviside's name for the quantity was adopted, his suggestion for the unit was rejected. This was the mac (plural max), which would give the reciprocal unit cam, and would suitably honour both ' the man who knew something about self-induction ' and his university.

A. L. MEYERS.

T.C. & M. Co., Ltd.
Greenwich, S.E.10.

ELECTRONIC APPLICATIONS

The Electronic Section of the Scientific Instrument Manufacturers' Association of Great Britain Ltd., is holding a symposium on the applications of electronics in research and industry at which the following papers will be read :—

The Measurement of Displacement by Electronic Method.
A Review of Frequency Measurement.
Electronics in Computing.
Measurement of Ionising Radiation.
High Vacuum Gauges.
The Radio Sonde and its Applications.
The Industrial Applications of Ultrasonics.
Metal Detection in Industry.
Electronic Control of Batching.
Electronics in Spectroscopy and Spectrophotometry.
Dynamic Recording of Mechanical Strains.
Picture Telegraphy.

The symposium is to be held at Caxton Hall, Westminster on 18th and 19th November. Tickets of admission are obtainable from the Secretary at 26, Russell Square, London, W.C.1.

BIRMINGHAM TELEVISION STATION

The B.B.C. has announced that the television transmitters being erected at Sutton Coldfield, near Birmingham, will operate on frequencies of 61.75 Mc/s (vision) and 58.25 Mc/s (sound) with powers of 35 kW and 12 kW respectively. A single aerial supported by a 750-ft mast will be used.

With one exception the signal characteristics will be the same as those of the London station. Amplitude modulation is retained for the sound channel and the present vision standards in waveform and frequency response will be adhered to. The exception is the adoption of semi-single sideband transmission on the vision channel. To conserve bandwith, the upper sidebands are to be partially suppressed.

WIRELESS PATENTS

A Summary of Recently Accepted Specifications

The following abstracts are prepared, with the permission of the Controller of H.M. Stationary Office, from Specifications obtainable at the Patent Office, 25, Southampton Buildings, London, W.C.2, price 1/- each.

DIRECTIONAL AND NAVIGATIONAL SYSTEMS

593 798.—Balancing arrangements for direction finders using Adcock aerials which are coupled through cathode-follower stages to their respective feed-lines.

Amalgamated Wireless (Australasia) Ltd. Convention date (Australia) 12th November, 1943.

593 892.—Radiolocation indicator in which the signal-traces presented to a rotating time base are progressively increased in intensity from the centre outwards.

W. A. Baker and C. Sharpe. Application date 19th June, 1945.

593 992.—Method of slicing and reshaping electric impulses, in order to measure their amplitude-duration, and build-up time, say in radiolocation.

Standard Telephones and Cables Ltd. (assignees of E. Labin and D. D. Grieg). Convention date (U.S.A.) 15th May, 1943.

594 239.—Radiolocation system, with means for measuring the rate-of-change of range, so as to indicate the relative speed of an observer and a target.

Western Electric Co. Inc. Convention date (U.S.A.) 21st March, 1944.

594 288.—Navigational system in which timed pulses radiated from three spaced beacons indicate the course and position of an aeroplane in flight.

Marconi's W.T. Co. Ltd. (assignees of E. I. Anderson). Convention date (U.S.A.) 2nd November, 1942.

594 346.—Radio-altimeter wherein the outgoing wave is modulated both in frequency and phase, and is constantly compared with its reflected counterpart.

J. H. Mitchell. Application date 6th May, 1944.

594 382.—Generating composite sweep or strobing voltages for the time base of a cathode-ray indicator, say for radiolocation.

Standard Telephones and Cables Ltd. (assignees of F. W. Frink). Convention date (U.S.A.) 9th August, 1944.

594 483.—Radiolocation system in which the echoes from successive exploring pulses are opposed in the receiver, in order to distinguish fixed from moving objects.

H. Grayson, D E. Brown and G. C. Barker. Application date 24th March, 1945.

594 484.—Steering-control indicator, say of an aeroplane making a blind-landing, which shows the off-course deviation, and also its rate-of-change.

H. C. Pritchard, F. C. Williams, and A. M. Uttley. Application date 20th April, 1945.

RECEIVING CIRCUITS AND APPARATUS

(See also under Television)

594 040.—Receiver for amplitude-modulated signals, provided with means for eliminating any interference that produces phase-modulation of the carrier wave.

W. S. Percival. Application date 23rd June, 1945.

594 622.—Adjustable resonant circuit of the concentric-line type, particular for use as an impedance-matching transformer, or input, to a receiver.

L. S. B. Alder, M. Slaffer, F. A. Mitchell and J. Buckingham. Application date 21st June, 1945.

594 711.—Filter-circuit, for use as a feedback path with a limited phase-drift, say in a bridge-stabilized oscillation-generator.

Standard Telephones and Cables Ltd., B. B. Jacobson and W. J. Mitchell. Application date 1st January, 1945.

TELEVISION CIRCUITS AND APPARATUS

FOR TRANSMISSION AND RECEPTION

594 327.—System for reproducing television pictures in natural colour at a high repetition-rate so as to reduce colour-flicker.

Farnsworth Television and Radio Corpn. Convention date (U.S.A.), 28th February, 1944.

594 786.—Mechanical scanning system for television in which auxiliary mirrors are used to multiply the rate of traverse without substantial loss of light.

Scophony Ltd. Convention date (U.S.A.), 24th February, 1944.

TRANSMITTING CIRCUITS AND APPARATUS

(See also under Television)

593 632.—Temperature-compensating device, including an auxiliary coil and conducting plate, say for the main circuit of an oscillation generator.

Marconi's W.T. Co., Ltd., and J. D. Brailsford. Application date 14th June, 1945.

594 368.—Filter-device, in the form of a conductive frame, adjustable in size and orientation, for use inside a waveguide.

Cie Generale de Telegraphie Sans Fils. Convention date (France), 14th December, 1943.

594 533 —Reactance-valve circuit including separate sections of transmission line, arranged for frequency-modulation.

Marconi's W.T. Co. Ltd. (assignees of R. W. Clark). Convention date (U.S.A.), 26th May, 1943.

SIGNALLING SYSTEMS OF DISTINCTIVE TYPE

593 694.—Detecting time-modulated signal-pulses by a method which involves frequency-conversion and re-shaping.

Standard Telephones and Cables Ltd. (communicated by International Standard Electric Corporation). Application date 20th October, 1944.

593 731.—Detecting time-modulated signal-pulses by first re-shaping and then converting them into an amplitude-modulated wave.

Standard Telephones and Cables Ltd. (assignees of E. Labin). Convention date (U.S.A.), 3rd July, 1942.

593 990.—Discriminating circuit for selecting pulses of a predetermined shape from others in radiolocation, television, or other signalling systems.

R. S. Webley. Application date 21st June, 1945.